THE TSR CHEMORECEPTOR/CHEW/CHEA TERNARY COMPLEX AS AN ALLOSTERIC ENZYME

A Thesis

by

LIN FAN

Submitted to the Office of Graduate Studies of
Texas A&M University
in partial fulfillment of the requirements for the degree of

MASTER OF SCIENCE

May 2006

Major Subject: Biochemistry

THE TSR CHEMORECEPTOR/CHEW/CHEA TERNARY COMPLEX AS AN ALLOSTERIC ENZYME

A Thesis

by

LIN FAN

Submitted to the Office of Graduate Studies of
Texas A&M University
in partial fulfillment of the requirements for the degree of

MASTER OF SCIENCE

Approved by:

Chair of Committee,	Gregory D. Reinhart
Committee Members,	Michael D. Manson
	Frank M. Raushel
	Dorothy E. Shippen
Head of Department,	Gregory D. Reinhart

May 2006

Major Subject: Biochemistry

ABSTRACT

The Tsr Chemoreceptor/CheW/CheA Ternary Complex as an Allosteric Enzyme.

(May 2006)

Lin Fan, B.S., Guangzhou University of Traditional Chinese Medicine;

M.S., Louisiana Tech University

Chair of Advisory Committee: Dr. Gregory D. Reinhart

The transmembrane serine receptor Tsr associates with a coupling protein, CheW, and a histidine kinase, CheA, to form a ternary complex that regulates the activity of CheA. CheA activity is inhibited by binding of L-serine to Tsr. This work aims to characterize the ligand-binding properties of Tsr and the inhibitory effect of L-serine on CheA activity. The periplasmic domain of Tsr (pTsr) was purified and characterized. Analytical gel filtration and analytical ultracentrifugation indicated that binding of L-serine promotes dimerization. The binding stoichiometry and dissociation constant for binding of L-serine to pTsr were determined by fluorescence spectroscopy. As protein concentration decreased, the dissociation constant increased. A working model was proposed to account for the interactions between L-serine and pTsr. The activity of CheA in a ternary complex with full-length Tsr and CheW was analyzed by measuring the production of [^{32}P]-phospho-CheY. (Phospho-CheY is the product of CheA catalysis.) The results revealed that binding of L-serine decreased CheA activity without changing its affinity for ATP. These findings suggest that the allosteric effect of L-serine on CheA

activity might occur through V-type inhibition. Optimization of an alternative, continuous, non-radioactive assay for CheA is underway.

DEDICATION

I would like to dedicate this work to my incredible family who has had the greatest influence on my life. They have shown me a world that has endless opportunities where all things are possible. They have always placed the highest expectations on me that have inspired me to be who I am today. They have given me unconditional love and for that I am forever grateful. They have respected and supported my decisions and have encouraged me throughout the highs and lows of the journey.

I thank my father for opening the opportunity to pursue my dreams. He was the rock that I could lean on. He was the beacon when I lost my direction in dark that he knew only so well from his travels before. What he provided me far exceeded what I could ever deserve.

I thank my mother for offering valuable encouragement and resources. She was always there listening patiently to my painful memories. It amazes me how she always knew just what to say when I was feeling down. I was always encouraged and ready to tackle the next obstacle after I put down the telephone.

I thank my sister for providing a remarkable model for me to follow. She showed me what is perseverance, and with it, I now know that I can accomplish anything. She gave me the strength that I needed, and without it, I would not have gone this far.

There is another "person" that I cannot leave out. He is my beloved baby dog, Boo Boo. He provided me joy that I could never get from elsewhere. He protected me from outside danger and licked my wound when I was hurt.

My passion towards my family is far beyond words. Without them, I would not have even tried to challenge myself and could not have completed this work. They were and will continue to be my greatest source of fulfillment and joy throughout life. I love my family so very much.

ACKNOWLEDGMENTS

So many people have helped to make this thesis a reality. I feel that it is almost impossible to acknowledge everyone that has contributed efforts.

Words cannot express how much I appreciate the generous assistance and support from my graduate committee. Each member provided guidance and encouragement in their own unique way. I owe special thanks to Dr. Gregory D. Reinhart, the chair of my committee, for his patience, endless encouragement, and support in the development of my ideas and for not giving up on me after I decided to pursue my professional life in a different direction. Tons of thanks are due to Dr. Michael D. Manson, an excellent mentor and a good friend for whom I have great respect. Thanks also go to two other committee members, Dr. Frank M. Raushel and Dr. Dorothy E. Shippen, for providing excellent scientific criticism. This thesis and my academic growth would not have occurred without them.

I greatly appreciate the technical support of Dr. Larry Dangott, Mr. Roger Draheim, Mr. Hongjun Jin, Mr. Renzhi Lai, Dr. Mauricio Lasagna, Dr. Michelle Lovingshimer, Dr. Jason Quinlan, Mr. Feng Wang, and Mr. Gus Wright. Many other members of the faculty, staff and graduate students at Texas A&M University, who enriched my academic life, also deserve my most sincere gratitude.

My appreciation is extended to everyone who it was my great honor to work with in the Reinhart's Lab. Special thanks to Dr. Michelle Lovingshimer and Dr. Monique

Parichartttanakul for agreeing to read this monster and Ms. Cuijuan Tie for being a great friend and colleague.

I also wish to thank my fellow graduate students in the Department of Biochemistry/Biophysics for providing me friendship and inspiration during my graduate study. I thank my dear friends that I made outside the department who lifted me up when I fell and cheered me on to the finish line.

I have received support, encouragement, and help from many who remain unnamed but also deserve recognition. You are all so special to me and I wish you all the happiness in the world.

NOMENCLATURE

Abbreviations

A	Substrate
ADP	Adenosine 5'-diphosphate
Aer	Cytoplasmic redox potential receptor
ATP	Adenosine 5'-triphosphate
BCA	Bicinchoninic Acid
D	Dimer
DNA	Deoxyribonucleic acid
DTT	Dithiothreitol
E	Enzyme
E_T	Total enzyme
E. coli	*Escherichia coli*
EDTA	Ethylenediaminetetraacetic acid
EPPS	N-[2-hydroxyethyl]piperazine-N'-[3-propanesulfonic acid]
IPTG	Isopropyl-thiogalactoside
KCl	Potassium phosphate (monobasic)
LB	Luria Bertani borth
Leu	Leucine
M	Molar or monomer
MES	2-[N-Morpholino]ethanesulfonic acid

MgADP	Magnesium adenosine 5'-diphosphate
MgATP	Magnesium adenosine 5'-triphosphate
$MgCl_2$	Magnesium chloride
MW	Milliwatt
MWC	Monod, Wyman and Changeux
NaCl	Sodium chloride
NAD^+	Nicotinamide adenine dinucleotide (oxidized form)
NADH	Nicotinamide adenine dinucleotide (reduced form)
$(NH_4)_2SO_4$	Ammonium sulfate
P	Product
PAGE	Polyacrylamide gel electrophoresis
PEP	Phospho(enol)pyruvate
pTsr	The periplasmic of Tsr
SDS	Sodium dodecyl sulfate
Ser	Serine
Tar	Transmembrane aspartate receptor
Tcp	Transmembrane citrate receptor protein
Trp	Transmembrane ribose and galactose receptor protein
Tsr	Transmembrane serine receptor
Tris	Tris[hydroxymethyl]aminomethane
X	Effector

Mathematical Terms

F	Relative steady-state fluorescence intensity
F^0	Maximal relative steady-state fluorescence intensity in the absence of effector
K_a	Michaelis-Menten constant or dissociation constants of L-serine binding to pTsr monomer
K_a^0	Michaelis-Menten constant in the absence of effector
K_a^{app}	Apparent dissociation constant of L-serine binding to pTsr
$K_{a/d}$	Dissociation constants of L-serine binding to pTsr dimer
K_d	Dissociation constants of pTsr monomer-dimer equilibrium in the absence of bound L-serine
$K_{d/a}$	Dissociation constants of pTsr monomer-dimer equilibrium in the presence of one bound L-serine per pTsr dimer
K_{ia}^0	Thermodynamic dissociation constant for A in the absence of effector
K_{ia}^∞	Thermodynamic dissociation constant for A in the saturating presence of effector
K_{ix}^0	Thermodynamic dissociation constant for X in the absence of substrate
K_{ix}^∞	Thermodynamic dissociation constant for X in the saturating presence of substrate
$K_{0.5}$	Concentration of substrate to produce half-maximal activity

kDa	Kilodalton
K_m	Michaelis-Menten constant
I	Intensity
mg	Milligram
mL	Milliliters
mM	Millimolar
n_H	Hill number
nm	Nanometers
Q	Coupling constant for the interaction between A and X
R	Gas constant
T	Temperature
U	Units
v	Initial velocity
V^0	Maximal velocity in the absence of effector
V_{max}	Maximal velocity
W	Coupling constant for the interaction between A and X which alters the maximal velocity
ΔG_a	Coupling free energy for the interaction between E and A in the absence of effector
$\Delta G_{a/x}$	Coupling free energy for the interaction between E and A in the saturating presence of effector

ΔG_x	Coupling free energy for the interaction between E and X in the absence of substrate
$\Delta G_{x/a}$	Coupling free energy for the interaction between E and X in the saturating presence of substrate
μL	Microliters
μM	Micromolar
μg	Microgram

TABLE OF CONTENTS

Page

CHAPTER Page

LIST OF TABLES

LIST OF FIGURES

FIGURE Page

CHAPTER I

INTRODUCTION

Many transmembrane receptors can be viewed as allosteric enzymes in which the regulatory site is extracellular and the catalytic site is in the cytoplasm. In *E. coli*, these transmembrane receptors typically contain a periplasmic N-terminal input domain and a cytoplasmic C-terminal signaling domain. These domains are connected by a transmembrane helix, known as TM2. External stimuli can be detected by the extracellular (or periplasmic, in Gram-negative bacteria) domain and transmitted across the cell membrane to the cytoplasmic domain to regulate the internal signaling machinery of the cell. As a result, structural, physiological, and behavioral changes can be triggered in response to changing environmental conditions.

Bacterial sensor kinases are one major type of transmembrane receptor. They are the input elements of two-component regulatory systems. The second component is a response regulator (RR), and some sensor kinases communicate with multiple RRs. Most sensor kinases detect an external stimulus and alter the activity of the cognate RR by phosphorylating it. The phosphorylated RR typically binds to DNA to activate or repress transcription. One well-studied sensor kinase is *E. coli* EnvZ, an osmosensor (Jin and

---

This thesis follows the style and format of *Biophysical Journal.*

Inouye, 1993). EnvZ and its cognate RR, OmpR, regulate the expression of outer-membrane porins in response to medium osmolarity.

Bacterial chemoreceptors are another example of this type of transmembrane signaling protein. Interaction of ligands with chemoreceptors ultimately regulates the clockwise/counterclockwise (CW/CCW) bias of the flagellar motors, and hence controls cellular locomotion. Chemotaxis allows cells to move towards more-favorable environments and away from less-favorable environments. Like sensor kinases, chemoreceptors are type I membrane receptors that typically function as homodimers. Chemoreceptors also belong to two-component regulatory systems. However, instead of having intrinsic kinase activity, like EnvZ, chemoreceptors function as regulatory subunits of a soluble kinase, CheA, which phosphorylates the CheY RR. Unlike typical RRs, phosphorylated CheY binds to the flagellar motor to promote CW rotation.

Why is it valid to think of chemoreceptors and their associated signaling proteins as allosteric enzymes? A ligand-binding site in the periplasmic domain of the receptor can be thought of as a regulatory site, and the ATP- and CheY-binding sites of CheA correspond to the active site of an allosteric protein. Chemoreceptors have not traditionally been viewed as allosteric proteins, since an allosteric protein is one in which the binding of a ligand to one site affects the binding properties of another site on the same protein. Nevertheless, when the chemoreceptor/CheW/CheA complex is considered as a unit, it can be viewed as one large allosteric protein. Thus, the behavior of the entire complex may be interpreted using allosteric mechanisms.

The rest of this chapter will introduce the background of bacterial chemotaxis, characteristics of the two abundant chemoreceptors, Tar and Tsr, regulation of chemotaxis, as well as models for allosteric regulation and chemotaxis.

Bacterial Chemotaxis

Bacterial chemotaxis is one of the most-studied model systems for signal transduction (Bren and Eisenbach, 2000; Bourret and Stock, 2002). Bacteria can respond to a variety of environmental parameters, including pH (Tso and Adler, 1974), temperature (Maeda et al., 1976), redox potential (Bibikov et al., 1997; Rebbapragada et al., 1997), amino acids (Mesibov and Adler, 1972), sugars (Adler et al., 1973), small peptides (Manson et al., 1986), and noxious organic compounds and divalent cations (Tso and Adler, 1974). Cells swim toward higher concentrations of attractants and away from higher concentrations of repellents (Adler, 1969) by biasing the three-dimensional random walk (Berg and Brown, 1972) that they exhibit in isotropic chemical environments. The random walk is generated by the alternation of smooth swims (or runs) in gently curved paths with abrupt, reorienting tumbles. The runs correspond to counterclockwise (CCW) flagellar rotation, and the tumbles correspond to clockwise (CW) flagellar rotation (Silverman and Simon, 1974). Spatial gradients are detected by a temporal comparison of concentration that is continuously updated as the cells swim (Macnab and Koshland, 1972; Brown and Berg, 1974).

Attractants and repellents are sensed by chemoreceptors, which are also known as methyl-accepting chemotaxis proteins (MCPs). *E. coli* has five chemoreceptors that

sense various repellents and the following attractants: Tar (aspartate and maltose), Tsr (serine), Tap (dipeptides), Trg (ribose, galactose, and glucose), and Aer (oxygen and other electron acceptors) (See Stock and Surette, 1996 for a review). Tap, Trg and Aer are low-abundance receptors that present at about 10% of the cellular levels of Tsr and Tar (Koman et al., 1979).

The basic functional unit of a chemoreceptor is a homodimer (Milligan and Koshland, 1988). Homodimers typically form clusters in association with the soluble chemotaxis (Che) proteins at the cell poles (Maddock and Shapiro, 1993). Chemicals in the environment are monitored by the periplasmic ligand-binding domains of the chemoreceptors, and the cellular response is mediated by their cytoplasmic signaling domains (Falke and Hazelbauer, 2001). The sequence of the signaling domain is highly conserved among chemoreceptors and interacts with the SH3-like coupling protein (CheW) and histidine kinase CheA (Borkovich et al., 1989; Gegner et al., 1992) (Figure 1-1). In the presence of ATP, CheA autophosphorylates, and the phosphoryl group is then transferred to a response regulator (CheY) to form phosphorylated CheY (CheY-P) (Stock et al., 1988; Hess et al., 1988a). CheY-P can be dephosphorylated by CheZ, a specific phosphatase (Hess et al., 1988b). CheY-P diffuses through the cytoplasm to the flagellar rotary motor to promote CW rotation of the flagellar filaments (Ravid et al., 1986; Welch et al., 1993), which are left-handed helices. CCW rotation coalesces the flagellar filaments into a bundle that propels the cell in a run, and CW rotation of one or more flagella disrupts the bundle to promote a tumble (Turner et al., 2000).

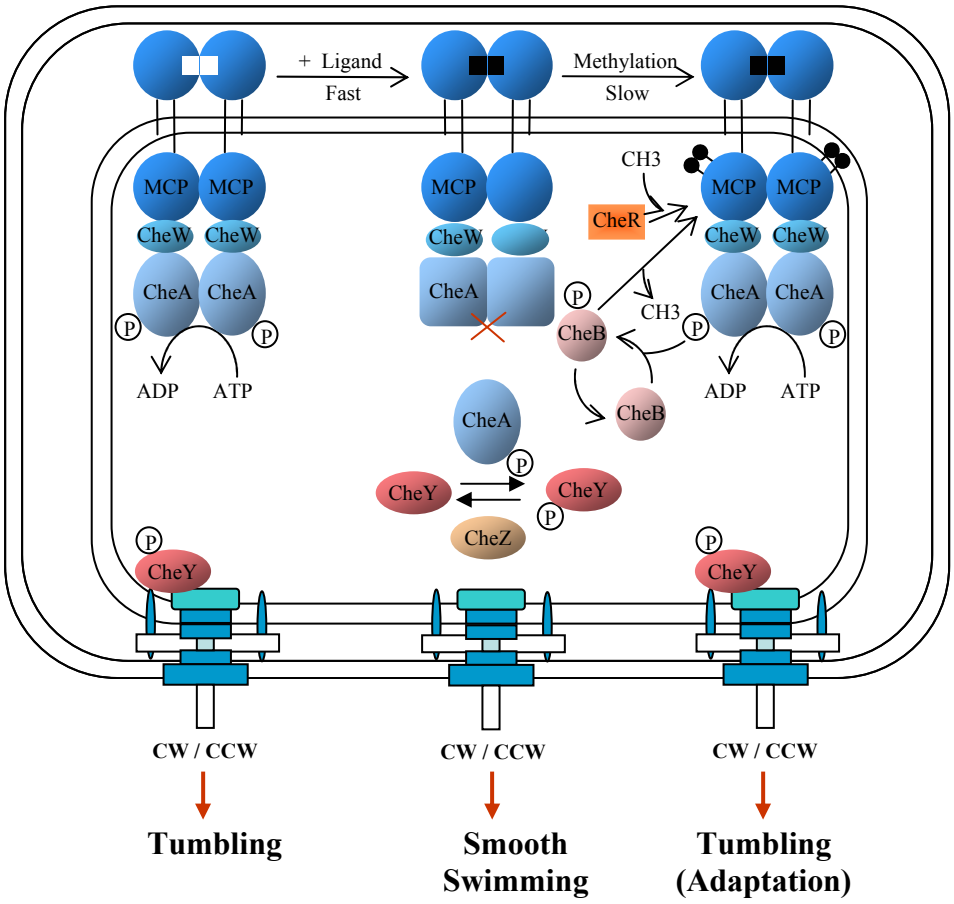

FIGURE 1-1: Chemotaxis system in *Escherichia coli* and *Salmonella typhimurium*. Methyl-accepting chemotaxis proteins (MCPs) form complexes with the SH3-like coupling protein (CheW), the histidine kinase (CheA), and the response regulator (CheY). In the presence of ATP, CheA autophosphorylates at a conserved histidyl residue, and the phosphoryl group is subsequently transferred to CheY. Phosphorylated CheY (CheY-P) then diffuses to and binds the switch component of the flagellar rotary motor and promotes a change from CCW to CW rotation. As a consequence, the bacteria begin tumbling. Ligand binding, the CheZ phosphatase, and the adaptation proteins (the CheR methyltransferase and the CheB methylesterase) regulate the production and destruction of CheY-P directly or indirectly. (See Stock and Surette, 1996, and Falke and Hazelbauer, 2001, for details and a general review.)

The pattern of bacterial movement depends on the cellular ratio of CheY to CheY-P (Cluzel et al., 2000), which is established by the relative activities of CheA and CheZ (Hess et al., 1988a). Chemoreceptors generally stimulate the activity of CheA (Borkovich et al., 1989). Binding of an attractant induces a conformational change in the receptor and switches it from being an activator of CheA activity to being an inhibitor (Borkovich and Simon, 1990). The sub-second motor response is followed by a slower adaptive response, which allows the bacterium return to its pre-stimulus run-tumble behavior (Macnab and Koshland, 1972; Berg and Brown, 1974; Berg and Tedesco, 1975; Segall et al., 1986). The adaptive response is modulated by receptor methylation (Goy et al., 1977). Cells respond similarly to decreasing concentrations of repellent as to increasing concentrations of attractant (Berg, 1975). Bacterial chemotaxis is highly sensitive, as is demonstrated by significant cellular responses to nanomolar concentrations of aspartate (Mao et al., 2003). A 35% inhibition of CheA kinase activity requires only a 1% increase in receptor occupancy by an attractant (Sourjik and Berg, 2002).

Tar and Tsr

Chemotaxis is commonly studied using the two high-abundance receptors, Tar and Tsr (Clarke et al., 1979). Sequence comparison of *E. coli* Tar and Tsr shows that the full-length proteins share 58% sequence identity. Tar is a dimer, even in the absence of aspartate, in detergent solution, in a mixed-micelle system, and in reconstituted membrane vesicles (Milligan and Koshland, 1988). *E. coli* Tar exhibits a very strong

negative cooperativity for aspartate binding (Biemann and Koshland, 1994), and *Salmonella* Tar and *E. coli* Tsr exhibit a less extreme negative cooperativity for aspartate binding (Biemann and Koshland, 1994) and serine binding (Lin et al., 1994), respectively.

Because of the difficulty of purifying and working with membrane-bound proteins, the extracellular portions of a number of receptors have been expressed and studied. This approach was first reported by Johnson et al. (1988) with human insulin receptor. The solublized extracellular portion of this receptor formed a heterotetramer similar to that observed with the full-length protein. Similar approaches were used with epidermal growth factor (Basu et al., 1989), the interleukin-1 receptor (Dower et al., 1989), the platelet-derived growth factor receptor (Duan et al., 1991), and the nerve growth factor receptor (Vissavajjhala and Ross, 1990). In all cases, the ligand affinities of the isolated binding domains were similar to those of their full-length cognates.

Milligan and Koshland (1993) purified and characterized the periplasmic domain of the aspartate chemoreceptor (Tar) from *Salmonella enterica serovar typhimurium*. The aspartate-binding affinity of this protein was determined to be 2 μM, a value consistent with that of purified full-length receptor (Clarke and Koshland, 1979; Foster et al., 1985). At protein concentrations below 5 μM, the periplasmic domain of Tar was predominantly monomeric in the absence of aspartate, whereas at 250 μM it was primarily dimeric. At any protein concentration, addition of a saturating concentration of aspartate induced dimerization by increasing the subunit affinity at least 100-fold.

The periplasmic domain of Tar has a single tryptophanyl residue at position 57. The sensitivity of this tryptophanyl residue to aspartate binding was tested, and an approximately 8% increase in fluorescence emission between 320 and 340 nm was observed after addition of 1 mM aspartate (Milligan and Koshland, 1993). This tryptophanyl residue, which is also present in Tsr, provides a convenient approach to study ligand binding properties.

The crystal structure of the periplasmic domain of Tar was determined in the absence (apo) and presence (complex) of aspartate (Milburn et al., 1991; Yeh et al., 1993; Yeh et al., 1996) (Figure 1-2). The periplasmic domain of Tar is a dimer of two four-helix-bundle subunits. There are two rotationally symmetric binding sites for L-aspartate per receptor dimer. Both binding sites are at the membrane-distal apex of the domain. The two binding sites are identical in the apo form. Aspartate binding at one site induces a rigid-body rotation between the two subunits and interrupts the symmetry (Yeh et al., 1996). When the crystals were grown with equal molar aspartate, only one aspartate was bound per dimer (Milburn et al., 1991; Yeh et al., 1993). The second binding site can be filled with a large excess of aspartate, but no further conformational changes occur (Yet et al., 1996). This result is in keeping with the negative cooperativity for aspartate binding exhibited by *Salmonella* Tar (Bieman and Koshland, 1994).

Regulation of Chemotaxis

In a chemoreceptor ternary complex, CheW physically connects the receptor with the CheA kinase (Gegner et al., 1992). The presence of CheW is required to couple

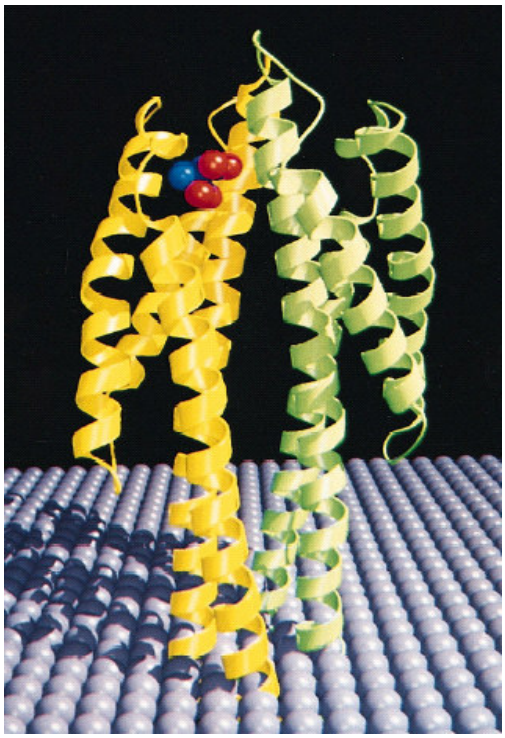

FIGURE 1-2: X-ray crystal structure of periplasmic domain of Tar. The crystal structure of the complex between an aspartate (shown as van der Waals atoms) and the ligand-binding domain of *Salmonella* Tar (one subunit show as a yellow ribbon, the other as a green ribbon) (Yeh et al., 1996). The polar head groups of the outer leaflet of the cell membrane are shown as a sheet of purple balls.

CheA with the receptor to allow activation of kinase activity but not to allow CheA to bind to the receptors (Ames and Parkinson, 1994; Borkovich et al., 1989; Gegner et al., 1992). The interactions between these proteins greatly alter the kinase activity of CheA. Upon formation of a ternary complex, an approximately 100-fold increase in CheA kinase activity was observed with Tsr and a 50-fold increase was observed with Tar (Lai et al., 2005). The kinase activity of CheA is regulated both by non-covalent ligand binding to the receptor and the covalent methylation of the receptor induced by ligand binding. Attractant binding to receptor-coupled CheA inhibits kinase activity to a level 5-fold below the activity of free CheA (Borkovich et al., 1989).

Methylation and demethylation of the MCPs involve the products of the *cheR* and *cheB* genes, respectively. CheR is a methyltransferase that catalyzes the methyl-esterification of four highly conserved glutamyl residues in the cytoplasmic portion of the receptors, using S-adenosylmethionine as the methyl donor (Stock and Stock, 1987). CheB is a methylesterase that hydrolyzes the methylesters formed by CheR (Stock et al., 1990). CheB is another substrate of CheA (Hess et al., 1988a), which activates CheB by phosphorylation (Lupas and Stock, 1989). Attractant binding to a receptor increases the rate of its methylation by CheR and inactivates CheB, resulting in an increased level of receptor methylation that reverses the inhibition of CheA kinase activity (Goy et al., 1977; Toews et al., 1979; Kehry et al., 1984). Receptor methylation decreases the sensitivity of bacteria to attractants (Li and Weis, 2000; Falke and Hazelbauer, 2001). The rapid inhibition of CheA activity induced by attractant binding transiently increases smooth swimming, enabling movement up an attractant gradient, whereas the slow,

methylation-dependent activation of CheA enabled by receptor methylation allows adaption to pre-stimulus behavior even though the attractant concentration remains high (Macnab and Koshland, 1972; Brown and Berg, 1974). Although previous research suggests that receptors signal via conformational changes in the ternary complex (Gegner et al., 1992), the molecular mechanism by which ligand binding and methylation are coupled to the control of kinase activity is not yet elucidated.

Chemoreceptors typically form clusters near the cell poles (Maddock and Shapiro, 1993). Accumulating evidence suggests that intermolecular communication among receptors in a cluster may play an important role in chemotaxis (Shimizu et al., 2000) and be responsible for the large gain in detection sensitivity (Gestwicki and Kiessling, 2002). The crystal structure of the cytoplasmic domain of Tsr reveals that three dimers of the Tsr cytoplasmic domain associate at their membrane-distal tips to form dimer of trimers (Kim et al., 1999). In addition, *in vitro* studies indicate that multiple receptors or receptor signaling domains are required for the activation and regulation of the CheA activity, although the optimal stoichiometries vary from system to system (Ames and Parkinson, 1994; Liu et al., 1997). Moreover, high-abundance and low-abundance receptors cooperate in regulating methylation during adaptation (Hazelbauer et al., 1989; Li et al., 1997; Weerasuriya et al., 1998; Feng et al., 1999). The intermolecular communication is further supported by the observation that receptors in ternary complexes exhibit positive cooperativity in the inhibitory effect on CheA activity upon attractant binding (Bornhorst and Falke, 2000; Li and Weis, 2000).

Models for Allosteric Regulation

Allosteric regulation is achieved through conformational alterations induced by the binding of ligands to allosteric sites that are distinct from active sites. The ligand that induces the changes in enzyme conformation, and hence activity, is called an allosteric effector. This type of regulation can be classified into two types: V-type and K-type. When the conformational changes associated with allosteric ligand binding cause an increase or decrease in the substrate binding affinity, the regulation is called K-type. V-type regulation occurs when an allosteric effector affects the specific activity of the enzyme. Both types of response can be induced by the same effector, and these effects need not be in the same direction (Reinhart, 2004). For example, the binding of an allosteric effector can increase the binding affinity for the substrate to the enzyme (K-type activation) while decreasing the catalytic activity (V-type inhibition). Most allosteric enzymes are regulated by altering their substrate binding affinity (K-type) (Reinhart, 2004).

Based on the nature of the ligand that causes the allosteric effect, allosteric regulation can also be separated into homotropic and heterotropic regulation. When the effecter is identical to the normal ligand or substrate of the protein, homotropic effects, which lead to cooperativity, are observed. Cooperativity is a common characteristic of most oligomeric allosteric proteins and can be observed as a change in ligand binding affinity as the concentration of the ligand increases. When the first binding event increases the binding affinity associated with the second interaction, it is called positive cooperativity. An example can be found in hemoglobin, a homotetramer containing one

oxygen-binding site in each subunit (Harkness, 1971). Binding of the first oxygen increases the affinity of subsequent oxygen binding to other sites. Negative cooperativity is observed when the binding affinity for the second ligand is decreased by the binding of the first. When there is no cooperativity, the same affinity is observed for the first and second binding interactions.

Unlike homotropic interactions, heterotropic effects occur when increases or decreases in substrate binding are caused by an allosteric effector that is different from the substrate and that binds at a distinct binding site.

The molecular mechanisms that underlie the phenomena of allostery are not yet completely understood. There are two classic models that describe the allosteric properties of enzymes, the Monod-Wyman-Changeux (MWC) (Monod et al., 1965), or concerted model, and the Koshland-Nemethy-Filmer (KNF) (Koshland et al., 1966), or sequential model (Figure 1-3). In both models the subunits of an allosteric enzyme undergo transition between two conformational states, the "taut" state (T state) and the "relaxed" state (R state). The T state is the inactive form and the R state is the active form. In these models, the substrate binds more tightly to the R state than to the T state.

According to the MWC model, an allosteric protein has multiple subunits that are functionally identical. The R state and T state are in equilibrium regardless of the number of bound substrates. In the presence of an activator, the equilibrium shifts toward the R state, whereas in the presence of an inhibitor the equilibrium shifts toward T state. Substrate binding promotes the T$\rightarrow$R transition in a concerted manner. While

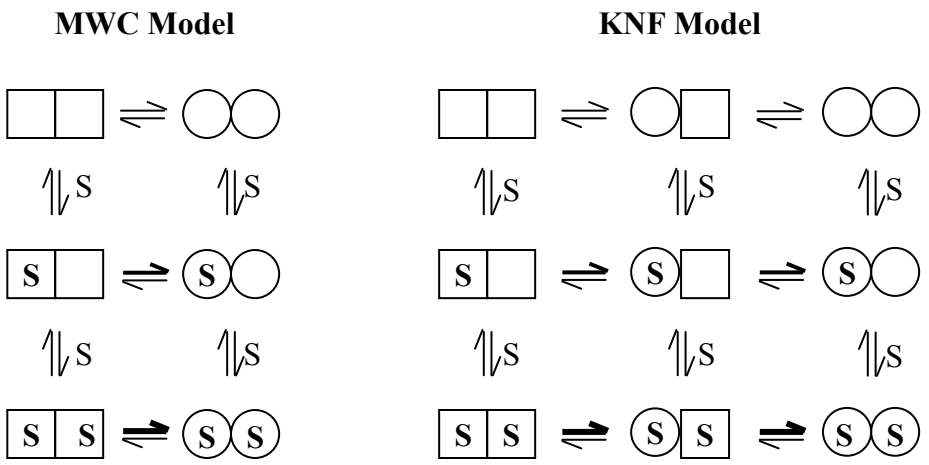

FIGURE 1-3: Schematic diagram of the MWC and KNF model for allosteric regulation of a dimeric protein. Squares and circles represent T- and R-state subunits, respectively. The substrate is represented by S.

elegant in its simplicity and capable of explaining activation, inhibition, and positive cooperativity, the MWC model cannot explain negative cooperativity.

The KNF model suggests that substrate binding induces the T→R transition only in the subunit to which the substrate binds and that it only influences the conformational changes on the neighboring subunits. The substrate binding affinity in these vacant subunits might be increased or decreased, depending on the induced conformational change. The T→R transition occurs sequentially as more substrate molecules bind to additional subunits. When all substrate binding sites are occupied, all subunits adopt the R state.

Although KNF model successfully accounts for all allosteric processes including negative cooperativity, it fails to consider the implications of the fact that both an allosteric effector and substrate may bind the enzyme simultaneously. A more complete quantitative analysis, based on linked-function thermodynamics, was proposed to describe allosteric regulation (Reinhart, 1983; Weber, 1972; Weber, 1975; Wyman, 1964; Wyman, 1967). In this scheme, the binding of an allosteric effector (X) and substrate (A) to an enzyme (E) to form a ternary complex (X-E-A) is described as:

$$E + A + X \rightleftharpoons X\text{-}E\text{-}A \qquad [1\text{-}5]$$

Four binding evens may occur for the enzyme to proceed from the ligand-free to ternary complex:

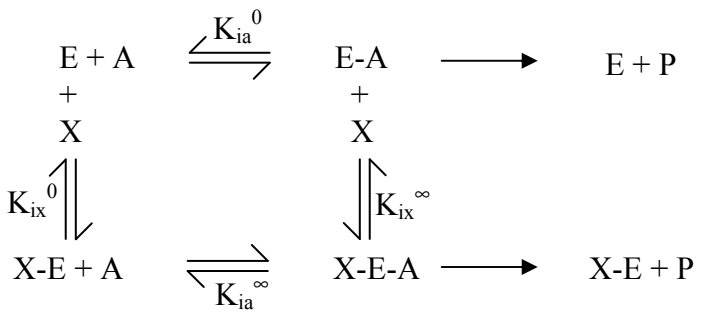

where K_{ia}^{0} is the dissociation constant for A binding to the enzyme in the absence of X, K_{ia}^{∞} is the dissociation constants for A binding to the enzyme when X is saturating, K_{ix}^{0} is the dissociation constants for X binding to the enzyme in the absence of A, and K_{ix}^{∞} is the dissociation constants for X binding to the enzyme when A is saturating. The binding free energy for each event can then be calculated as:

$$\Delta G_a = RT\ln K_{ia}^{0} \quad [1\text{-}6]$$

$$\Delta G_x = RT\ln K_{ix}^{0} \quad [1\text{-}7]$$

$$\Delta G_{a/x} = RT\ln K_{ia}^{\infty} \quad [1\text{-}8]$$

$$\Delta G_{x/a} = RT\ln K_{ix}^{\infty} \quad [1\text{-}9]$$

The total binding free energy should not depend on the path taken to the X-E-A ternary complex. Therefore,

$$\Delta G_a + \Delta G_{x/a} = \Delta G_x + \Delta G_{a/x} \quad [1\text{-}10]$$

Substituting equation [1-6] to [1-9] into equation [1-10] gives:

$$K_{ia}^{0} K_{ix}^{\infty} = K_{ix}^{0} K_{ia}^{\infty} \quad [1\text{-}11]$$

By rearranging equation [1-11], a coupling constant, Q, can be defined as follows:

$$Q = \frac{K_{ia}^{0}}{K_{ia}^{\infty}} = \frac{K_{ix}^{0}}{K_{ix}^{\infty}} \quad [1\text{-}12]$$

where the coupling constant, Q, represents the degree to which effector changes substrate binding affinity, or vice versa. If $Q < 1$ the allosteric effector is an inhibitor, if $Q > 1$ the allosteric effector is an activator, and if $Q = 1$ the allosteric effector has no effect on substrate binding.

Assuming that the substrate is in rapid equilibrium (Frieden, 1964) or that the allosteric ligand achieves a binding equilibrium in the steady-state (Reinhart, 1983), the rate equation describing how a single allosteric ligand affects the initial velocity, v, of a single substrate is given by following equation:

$$\frac{v}{E_T} = \frac{V^0(K_{ix}^0[A] + QW[A][X])}{K_{ix}^0 K_a^0 + K_{ix}^0[A] + K_a^0[X] + Q[A][X]} \qquad [1\text{-}13]$$

where v is the initial velocity, E_T is the total enzyme concentration, V^0 is the maximal velocity when [X] = 0, and W is the ratio of maximal velocity when [X] = ∞ to [X]= 0. For a K-type effector, W=1. Based on Hill equation (Hill, 1910), when $v/E_T = V^0/2$, [A] = K_a. Then equation [1-13] can be re-written as:

$$K_a = K_a^0[\frac{K_{ix}^0 + [X]}{K_{ix}^0 + Q[X]}] \qquad [1\text{-}14]$$

Allosteric Model for Chemotaxis

Like other well-known allosteric proteins, the regulation of chemotaxis signaling may depend on the ability of protein molecules to change conformations in a reversible manner (Gegner et al., 1992). However, unlike hemoglobin or aspartate transcarbamylase (Monod et al., 1965; Koshland et al., 1966), the phenomenon of chemotaxis cannot be precisely explained by the MWC or KNF models (1-3). Descriptions of allostery using these two models have been confined to the spread of conformational states within a single multisubunit molecule. Therefore, neither of these models can explain the high sensitivity seen in chemotactic systems. Bray and Duke proposed another model termed conformational spread (CS) (Bray and Duke, 2004).

This model takes into account the possibility of conformational spread through large complexes, or clusters, composed of different or identical receptors. In the CS model, a conformational state is stabilized either by ligand binding or by the conformational state of the neighboring receptors. This model is consistent with the large signal amplification, or "gain", observed in chemotaxis (Bray, 2002) and the cross-talk between receptors of the same (Bray et al., 1998) and different (Gestwicki and Kiessling, 2002) types. Quantitative analysis of the system using linked-function thermodynamics offers a possible solution to explain the control of receptor function during bacterial chemotaxis.

Chapter Overview

Chapters II and III discuss the purification and characterization of the periplasmic domain of Tsr (pTsr). In Chapter II, two methods are used to test the oligomeric states of pTsr in the presence and absence of ligands. The focus of Chapter III is the determination of the binding stoichiometry and binding affinity of L-serine to pTsr. The binding properties of L-leucine and competition between L-serine and L-leucine are also addressed.

Chapter IV describes a study of the coupling between ligand binding to full-length membrane-bound Tsr and kinase activity of the Tsr/CheW/CheA ternary complex. The method used is a modified version of the receptor-coupled phosphorylation assay described by Borkovich and Simon (1991). The optimization of an alternative method for measuring the specific steady-state activity of CheA from the

spectroscopic pyruvate kinase/lactate dehydrogenase coupled assay described by Surette et al. (1996) is also described in this chapter.

The ultimate goal of this project is to understand the basic molecular mechanisms that underline the signal transduction pathway that mediates chemotaxis. This work should pave the way for a fuller understanding of the allosteric regulation in this unique signal transduction system.

CHAPTER II

CHARACTERIZATION OF THE PERIPLASMIC DOMAIN OF TSR - THE OLIGOMERIC STATE (PART I)

Tsr chemoreceptor is a membrane-bound protein with five distinct functional domains: the periplasmic sensing domain, two transmembrane segments, a linker region, and the cytoplasmic signaling domain (Milligan and Koshland, 1988; Kim et al., 1999). In order to study the properties of individual functional domains, it will be useful to study the properties of each functional domain in isolation. In this chapter, the purification process of the periplasmic domain of pTsr is addressed.

Chemoreceptor homodimers form trimers of dimers (Kim et al., 1999) and even higher-order receptor assemblies in the cell membrane. The aspartate chemoreceptor (Tar) and the serine chemoreceptor (Tsr) are closely related. They share 58% sequence identity overall, but only 34% sequence identity in their periplasmic domains. The periplasmic domain of Tar (pTar) has been shown to exist in a monomer-dimer equilibrium that is influenced by protein concentration and ligand-binding (Milligan and Koshland, 1993). At low protein concentrations or in the absence of aspartate, pTar is found predominantly as a monomer. An increase in protein concentration or the presence of aspartate shifts the equilibrium toward the dimer. It is possible that pTsr undergoes a similar monomer-dimer transition. To test this hypothesis, two biophysical techniques, analytical gel-filtration and analytical sedimentation-equilibrium ultracentrifugation, were used to address the oligomeric state of pTsr in the absence and presence of ligands.

Gel-filtration chromatography is a technique that separates biological macromolecules based on their size and shape. It has been widely used because it is inexpensive, easy to use, and gentle on the samples. Samples pass through a column filled with a bed of beads with a well-defined range of pore sizes. These beads are used as the stationary phase. Buffer, which flows through the column, constitutes mobile phase. Proteins elute in order of decreasing molecular weight in a gel-filtration column. Small molecules that can fit into the pores in the beads migrate through a larger volume and therefore come out of column last. Large molecules that cannot fit into the beads migrate between them and pass through first in the void volume (the volume of the mobile phase in a column). Intermediately sized proteins that can pass through only some of the pores elute at intermediate times.

One application of analytical gel-filtration chromatography is to estimate the apparent molecular mass, M, of a protein by calibrating the column using markers of known molecular mass before running the sample. According to the apparent molecular mass, one can determine the oligomeric state of a protein (Gupta et al., 2004). However, the apparent molecular mass estimated by analytical gel-filtration dependents on the shape of the protein. Therefore, other techniques are always used to confirm the measurement of the molecular mass of a protein.

Analytical ultracentrifugation is used for the determination of the hydrodynamic and thermodynamic parameters for associating systems. Sedimentation-velocity and sedimentation-equilibrium are two different types of analytical ultracentrifugation. Sedimentation-velocity is sensitive to the mass and shape of the macromolecules, so it is

used to determine the sedimentation coefficient, *s*, and the diffusion coefficient, *D*. Sedimentation-equilibrium is sensitive to the mass but not the shape of macromolecules, so it is used to determine the molecular mass.

In sedimentation-equilibrium experiments, the centrifugal field applied to the sample is high enough to allow the movement of the macromolecules towards the bottom of the centrifuge cell but low enough to prevent all the macromolecules from moving to bottom of the cell. Sample concentration is scanned and recorded as a function of the radial distance at different times. The initial concentration throughout the centrifuge cell is uniform. During centrifugation, the macromolecules start to deplete from the meniscus. Two opposing process, diffusion and sedimentation, eventually reach equilibrium throughout the cell. At equilibrium, the solute concentration increases exponentially towards bottom of the centrifuge cell, and there is no change in the distribution over time. For a single component, ideal system, the concentration distribution can be described by following equation:

$$c(r) = c_0 \exp[M(1-\nabla \rho)\, \omega^2(r^2-r_0^2)/2RT] \qquad [2\text{-}1]$$

where c(r) is the concentration at radial position r, c_0 is the concentration at the meniscus, and r_0 is the radial distance of meniscus. The molecular mass of macromolecules in single ideal systems can be calculated from the slope of the plot Log c(r) vs r^2, which is $M(1 - \nabla \rho)/2RT$.

The key advantage of sedimentation-equilibrium experiments is that the concentration distribution depends on the molecular mass of a macromolecule regardless of its shape. Therefore, this technique allows accurate determination of the molecular

mass of macromolecules without having to assume that they have a globular shape, as is required in gel-filtration chromatography. For self- or hetero-associating systems, apparent molecular masses greater than that of the monomer will be determined, and the oligomeric state of the macromolecule can be predicted accordingly.

Materials and Methods

Materials. All chemical reagents and buffers were of analytical grade and purchased from Fisher Scientific or Sigma-Aldrich. The HR 10/30 Superdex-G75 Column was purchased from Amersham Pharmacia Biotech for use on their Fast Performance Liquid Chromatography (FPLC) system. Protein standards, ribonuclease A (13.7 kDa), chymotrypsinogen (25.0 kDa), ovalbumin (43.0 kDa), and albumin (67.0 kDa) were purchased from Amersham Pharmacia Biotech. Sedimentation experiments were carried out using a CMD Beckman XL-A Analytical Ultracentrifuge.

Protein Purification. Purification of pTsr followed the protocol of Daniel et al. (1993) with some modifications. BL21 (DE3) cells containing the pTsr32-188 gene in plasmid pGEM-3Z were grown in 1.5 L LB broth containing 100 μg/mL ampicillin at 37 °C for 4 hours. Expression of pTsr was induced by adding 2 mM IPTG, and the cells were then grown for an additional 5 hours. Cells were harvested by centrifugation at 5,000 x g for 30 min using a Beckman Model J-6B centrifuge. Pelleted cells were stored at –20°C until ready for lysis. Frozen cell pellets were resuspended in approximately 30 mL of resuspension buffer (100 mM Tris-HCl [pH 8.0], 0.5mM EDTA) and lysed by sonication using a Sonic Dismembrator Model 550 (Fisher Scientific) with 15-sec pulses

for a total sonication time of 8 min. Cell debris was cleared by centrifugation at 25,000 x g for 30 min in a Beckman J2-21 centrifuge, using a JA-20 rotor. The supernatant was brought to 40% saturated ammonium sulfate and stirred on ice for 30 min. The solution was centrifuged at 25,000 x g for 30 min at 4°C. The supernatant was brought to 60% saturated ammonium sulfate and stirred on ice for 30 min. The proteins precipitated at 60% ammonium sulfate included pTsr and were collected by centrifugation at 4°C and 25,000 x g for 30 min.

The precipitate was resuspended in Buffer A (10 mM Tris [pH 8.0]) to a final volume 1~4% of the bed volume of the size exclusion column. The protein solution was filtered with 0.22 μm Millex-GV filter (Millipore) and then loaded onto a G-100 column that had been pre-equilibrated with Buffer A. The column was washed with Buffer A and fractions were collected. Each fraction was assayed for absorbance at 280 nm and visualized by SDS-PAGE (Laemmli, 1970).

Based on SDS-PAGE, fractions containing proteins of ~18.7 kDa, the molecular weight of a pTsr monomer, were pooled, filtered, and loaded onto a pre-equilibrated Mono Q column. Proteins were then eluted with a 0 to 200 mM NaCl gradient in 10 mM Tris [pH 8.0]. The absorbance of the column eluate was monitored at 280 nm and subjected to SDS-PAGE to locate pTsr. The identity pTsr was confirmed by N-terminal protein sequencing.

Originally, the purification proceeded by pooling the fractions containing pTsr and dialyzing against Buffer A (Procedure I). The sample was then filtered and loaded onto a Mono Q column preequilibrated with Buffer A. Proteins were eluted with a much

shallower NaCl gradient than was used for the first pass. Fractions with pure pTsr were pooled, concentrated using Amicon concentrators with an YM-10 membrane, and dialyzed against fluorescence buffer (25mM EPPS [pH 7.4]) at 4°C.

We found that changing the pH to 6.0 during the second pass over the Mono Q column could improve the final yield greatly (Procedure II). The fractions containing pTsr from the first pass were pooled and dialyzed against Buffer B (10 mM MES [pH 6.0]). The sample was filtered and loaded onto Mono Q column pre-equilibriated with Buffer B. Proteins were eluted with a 0 to 200 mM NaCl gradient. Fractions with pure pTsr were pooled, concentrated, and dialyzed against fluorescence buffer at 4°C. All the experiments described in this chapter used pTsr obtained by Procedure II.

Protein Concentration. Determination of protein concentration was performed using the Bicinchoninic Acid (BCA) Protein Assay (Smith et al., 1985). Alternatively, protein concentration was also calculated based on Beer's Law:

$$C=A/\varepsilon l \qquad [2\text{-}2]$$

where ε is the molar absorption coefficient ($M^{-1}cm^{-1}$), l is the pathlength (cm), and C is the protein concentration (M). The extinction coefficient of pTsr was determined by the Edelhoch method (Pace, 1995) to be 18827 $M^{-1}cm^{-1}$. The concentrations calculated by each method agreed with each other.

Analytical Gel-Filtration. Analytical gel-filtration chromatography was performed at 4°C using a HR 10/30 Superdex-G75 Column. The column was pre-equilibrated with sample buffer (25 mM EPPS [pH 7.4], 200 mM NaCl, and the indicated concentrations of ligand). Protein at 50 μM was dialyzed against sample buffer

containing ligand at different concentrations. Fifty μL of sample were loaded onto the column and eluted. The absorbance of the eluate was monitored at 280 nm. The apparent molecular weight of the eluate was estimated from a calibration curve generated by plotting the distribution coefficients (K_{av}) of protein standards against their molecular weight on a log scale, where K_{av} is defined as [(elution volume - void volume) / (column volume – void volume)]. The standards were run separately in the same buffer. The apparent molecular weights of samples were calculated from the linear relationship between K_{av} and log (MW) determined by the calibration curve.

Analytical Ultracentrifugation. Sedimentation-equilibrium experiments were carried out at 4°C. Protein concentrations varied from 3 μM to 70 μM. Samples contained L-serine at 0 mM, 1 mM, and 10 mM, respectively. Prior to centrifugation, the protein was dialyzed into 25 mM EPPS buffer [pH 7.4] containing 200 mM NaCl and the indicated concentration of ligand. Twelve mm double-sector Epon charcoal filled cells with quartz windows were loaded into an AN60Ti four-hole rotor. Samples were centrifuged at 15,000 RPM and the concentration gradient was recorded at 8 h intervals by absorbance optics. Samples were assumed to reach equilibrium when consecutive scans at 280 nm of the radial position taken at 2 h intervals were identical. Data were collected and analyzed after equilibrium had been reached.

Data Analysis. The data were fit to the single-species model using Kaleidagraph 3.5 (Synergy). This model allows the calculation of an apparent weight-average molecular mass in any system. The fitting equation used in this model is:

$$c(r) = c_0 \exp [H \cdot M (r^2 - r_0^2)] + E \qquad [2\text{-}3]$$

where c(r) is the absorbance at radius r, c_0 is the absorbance at reference radius r_0, exp is the exponent, H is the constant $(1-\nabla\rho)\omega^2/2RT$, ∇ is the partial specific volume of the macromolecule (mL/g), ρ is the density of the solvent (mL/g), ω is the angular velocity of the rotor (radius/sec)=2π x speed/60, E is the baseline offset, and M is the gram molecular mass of the macromolecule.

Results and Discussion

Purification. pTsr was purified in four steps: selective ammonium sulfate precipitation, gel-filtration chromatography, and two passes through an anion exchange column. Ammonium sulfate was first added to the crude extract to 40% saturation and precipitated many unwanted proteins (Figure 2-1). The ammonium sulfate concentration was then increased to 60% saturation to precipitate pTsr (Figure 2-1). The precipitate was solublized in buffer and introduced to the G-100 gel-filtration column. A few faint contaminant bands and two major bands were seen after SDS-PAGE (Figure 2-2). Anion exchange using a Mono Q10/10 column at pH 8.0 eliminated the faint contaminants, leaving two bands on SDS-PAGE (Figure 2-3), one of which had the apparent molecular weight expect for pTsr. The second band had an apparent molecular weight about twice as that of pTsr. N-terminal protein sequencing indicated that the lower band was pTsr and the upper band was β-lactamase, the periplasmic enzyme encoded by the vector plasmid that is responsible for bacterial resistance to β-lactam antibiotics, including ampicillin (data is not shown). A final step on the anion exchange column at pH 8.0

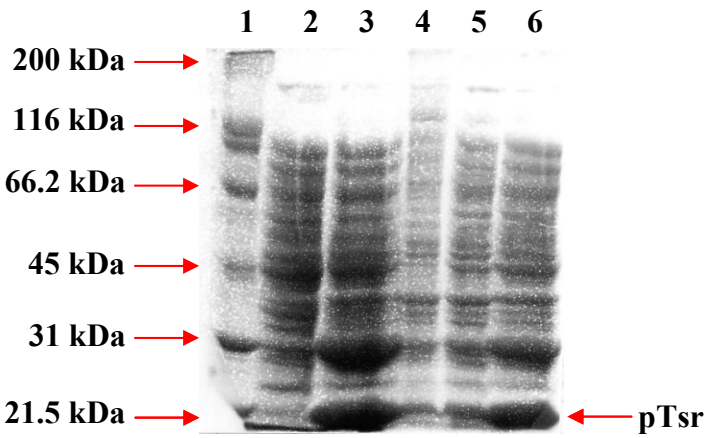

FIGURE 2-1: 12% SDS-PAGE of ammonium sulfate trial. Lane 1 contains the molecular weight markers. Lane 2 contains the lysate from cells without IPTG induction. Lane 3 contains the lysate from cells grown for 5 hours after induction with 2 mM IPTG. Lanes 4, 5, and 6 contain the resuspended pellet after precipitation with 35%, 45%, and 55% ammonium sulfate.

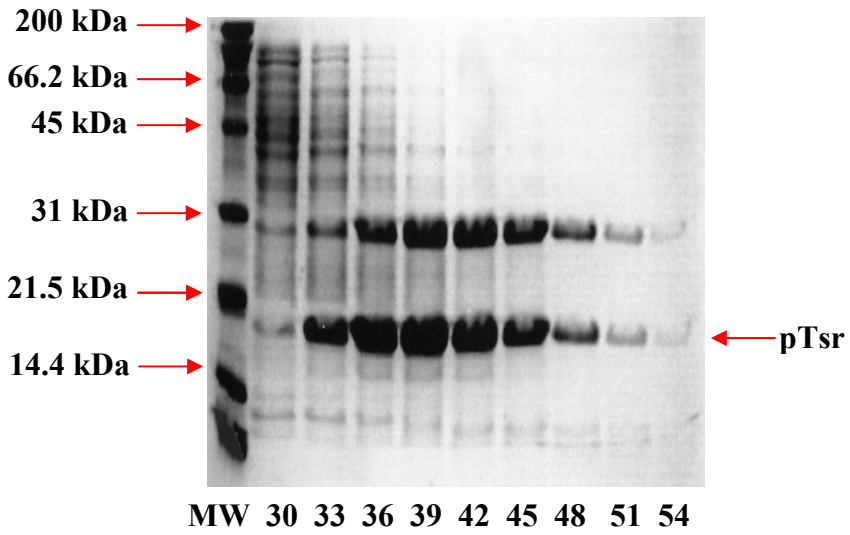

FIGURE 2-2: 17% SDS-PAGE of fractions from a G-100 gel-filtration column. The first lane contains the molecular weight markers. The other lanes contain the indicated fractions. Fractions 33 to 51 were pooled and loaded onto a Mono Q column.

A

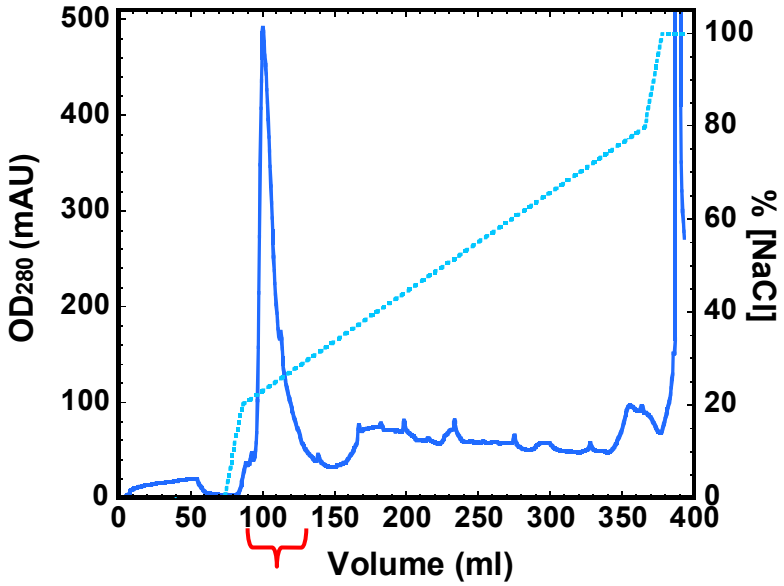

B

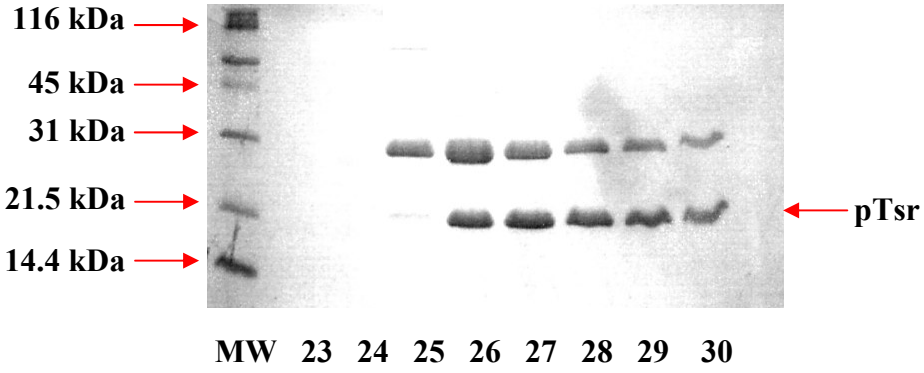

FIGURE 2-3: pH 8.0 Mono Q fractions. A) Elution profile of Tsr from the Mono Q. The absorbance profile at 280 nm is shown as a solid line, and the NaCl concentration gradient is shown as a dashed line. The bracket shows the fractions that were tested by SDS-PAGE. B) SDS-PAGE of fractions from Mono Q column. The first lane contains the molecular weight markers. The other lanes contain the indicated fractions. Fractions 25 to 30 were pooled, dialyzed against 10 mM MES buffer at pH 6.0, and loaded onto a second Mono Q column.

(Procedure I) (data not shown) or at pH 6.0 (Procedure II) (Figure 2-4) separated pTsr from β-lactamase. This procedure purified pTsr to homogeneity, as shown by SDS-PAGE. The final yield from 1 L of cell culture was approximately 10-20 mg of pure pTsr using Procedure II, about 20-fold higher than the yield from Procedure I.

Analytical Gel-Filtration. In the absence of ligand, the elution volume of pTsr corresponded to an apparent molecular mass equal to 25.5 kDa. This is approximately 1.4 times the theoretical molecular mass of a pTsr monomer, which is 18.7 kDa. The apparent molecular mass was calculated based on the standard curve (Figure 2-5) generated using proteins of known molecular mass. In the presence of L-serine, the apparent molecular mass increased. Higher L-serine concentrations resulted in higher apparent molecular masses (Figure 2-6). Apparent molecular masses of 29.0 and 36.7 kDa, respectively, were observed for samples containing 10 μM and 100 μM L-serine. When a saturating L-serine concentration (50 mM) was used, the apparent molecular mass was 39.6 kDa, which is about 2.1 times the theoretical molecular mass of a pTsr monomer. These results suggested that pTsr exists predominantly as a monomer in the absence of L-serine and dimerizes in the presence of the ligand. From the positions of the peaks in Figure 2-6, one can easily see that the longest transition in the apparent molecular mass occurs between 10 μM and 100 μM L-serine (peaks B and C). Sample with 50 μL of 50 μM protein were loaded onto the column. In each run, based on the peak volume, the protein was diluted approximately 10-fold on the column. Therefore, one can expect a dissociation constant (K_d) for L-serine in the range of 10 μM to 100 μM for 5 μM pTsr. Only a small change in the apparent molecular mass was observed

A

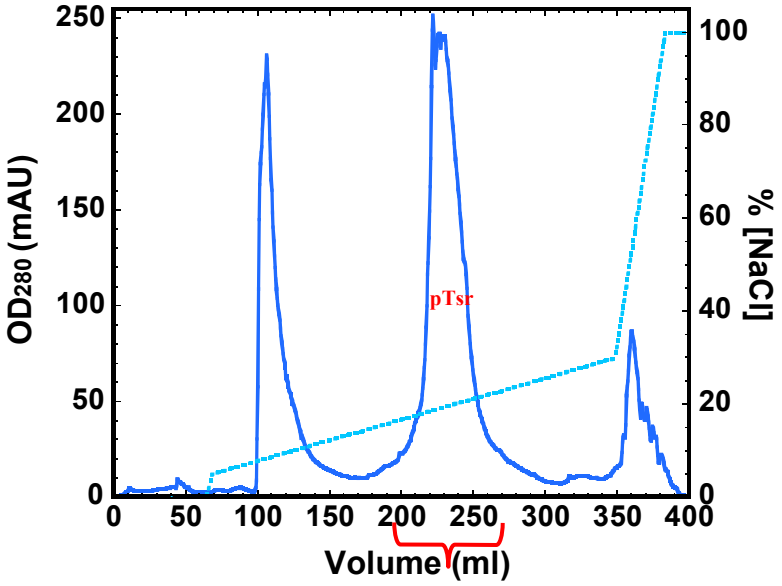

B

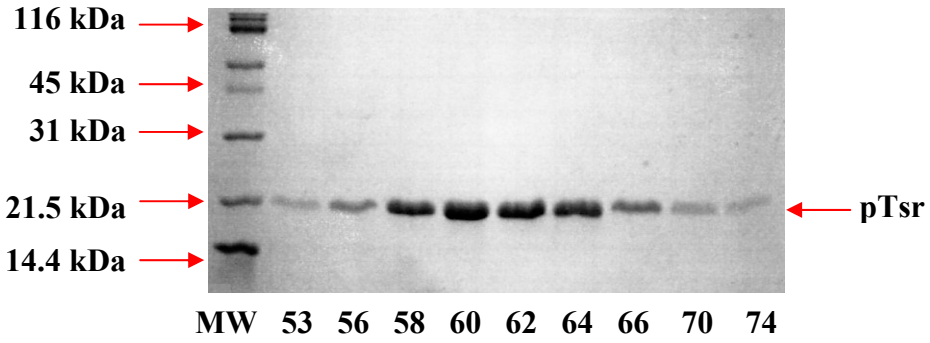

FIGURE 2-4: pH 6.0 Mono Q fractions. A) Elution profile of Tsr during a second pass over the Mono Q column. The absorbance profile at 280 nm is shown as a solid line and the NaCl concentration gradient is shown as a dashed line. The bracket shows the fractions that were tested by SDS-PAGE. B) SDS-PAGE of fractions from the Mono Q column. The first lane contains the molecular weight markers. The other lanes contain the indicated fractions. Fractions 53 to 74 were pooled, concentrated, and dialyzed against 25 mM EPPS buffer at pH 7.4 at 4°C.

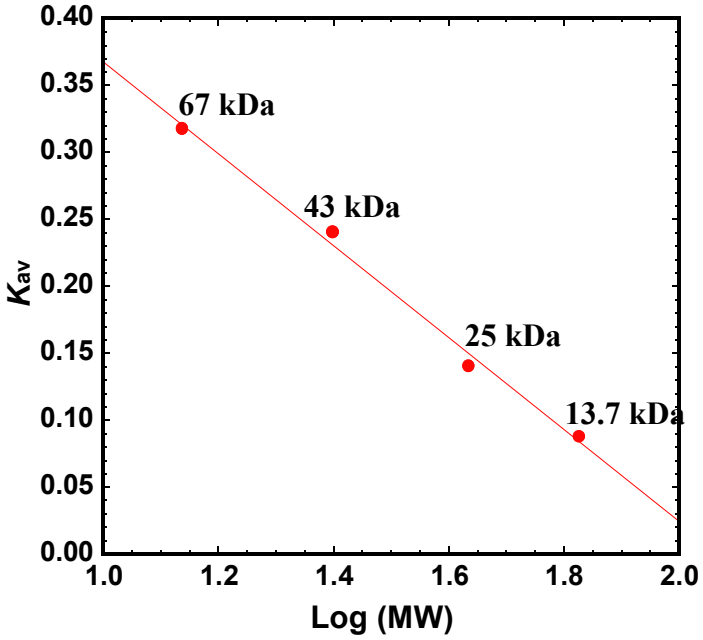

FIGURE 2-5: Standard curve obtained for the analytical gel-filtration column. The ability of the column to resolve pTsr monomers (18.7 kDa) from dimers (37.4 kDa) was tested by injecting ribonuclease A (13.7 kDa), chymotrypsinogen (25 kDa), ovalbumin (43 kDa), and albumin (67 kDa), separately, in 25 mM EPPS [pH 7.4] and 200 mM NaCl. The curve was generated by plotting the distribution coefficient *K*av of each protein against the log of its molecular mass.

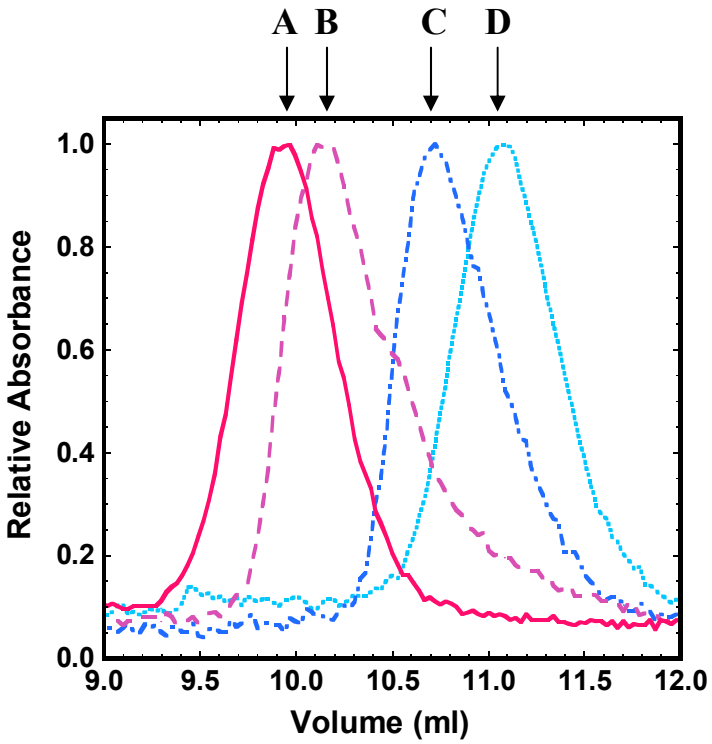

FIGURE 2-6: Gel-filtration chromatography data for pTsr– L-Serine. The elution profile for samples with 0 µM, 10 µM, 100 µM and 50 mM L-serine are shown as a dotted light blue line, dotted and dashed dark blue line, dashed purple line, and solid red line, respectively. The peaks correspond to apparent molecular mass as of: A) 39.6 kDa, B) 36.7 kDa, C) 29.0 kDa, and D) 25.5 kDa.

when 50 mM L-leucine was present (Figure 2-7). This small shift might be evidence of a very weak binding between L-leucine and pTsr.

Analytical Ultracentrifugation. Figure 2-8 shows a representative data set for samples without L-serine. The data were fit to a single-species model (equation [2-3]), and an apparent molecular mass of 20.6 ± 0.1 kDa for the protein was obtained. The residual indicates a good data fit. The value of the apparent molecular mass is close to, but slightly larger, than a monomer (18.7 kDa). Some pTsr dimmers may have existed in the solution to cause an increase in the apparent molecular mass. A representative data set for samples with 1 mM L- serine is shown in Figure 2-9. The concentration distribution shown in Figure 2-9 is steeper than that without ligand (Figure 2-8), indicating that pTsr may be self-associating. The data were fit to equation [2-3] and resulted in an apparent molecular mass of 32.5 ± 0.2 kDa, which is less than that of a dimer (37.4 kDa). A possible explanation is that L-serine promotes a shift of monomer-dimer equilibrium towards dimer but there is still a population of monomer present. These experiments were repeated at two different experimental temperatures and with different protein and ligand concentrations. All of the results are summarized in Table 2-1. In the absence of L-serine, the molecular masses estimated for all conditions are most consistent with pTsr existing primarily as a monomer. When the apparent molecular mass was plotted as a function of pTsr concentration (Figure 2-10), the apparent molecular mass clearly shifted towards a pTsr dimer in the presence of L-serine. Samples with L-serine concentrations of 1 mM and 10 mM had similar apparent molecular masses. However, no increase in the apparent molecular mass was observed

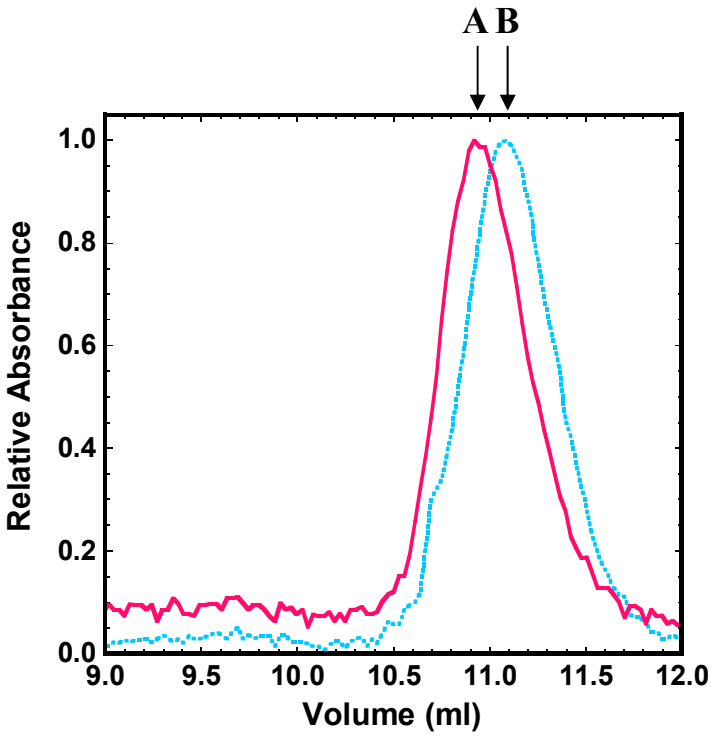

FIGURE 2-7: Gel-filtration chromatography data for pTsr– L-leucine. The elution profile for samples with 0 mM and 50 mM L-leucine are shown as a dotted light blue line and a solid red line, respectively. The peaks correspond to apparent molecular mass as of: A) 26.3 kDa and B) 25.5 kDa.

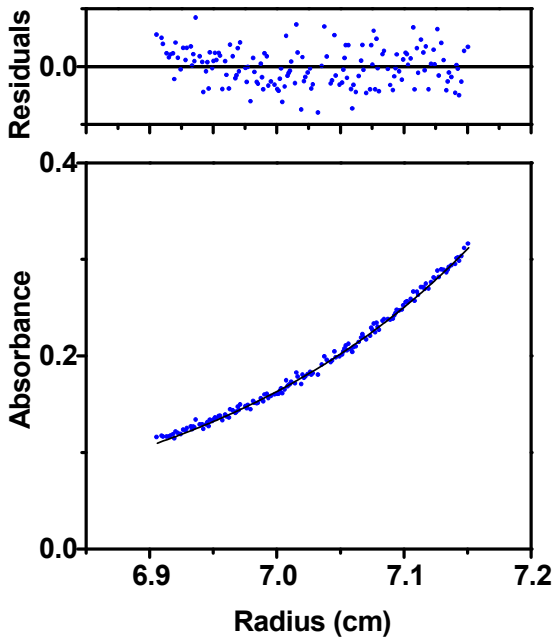

FIGURE 2-8: Sedimentation-equilibrium data for pTsr in the absence of ligand. The sample contained 8 μM pTsr. Data are shown as closed circles. The smooth curve represents a nonlinear fit to equation [2-3]. The residuals are shown in the upper panel. The average molecular mass obtained was 20.6 ± 0.1kDa.

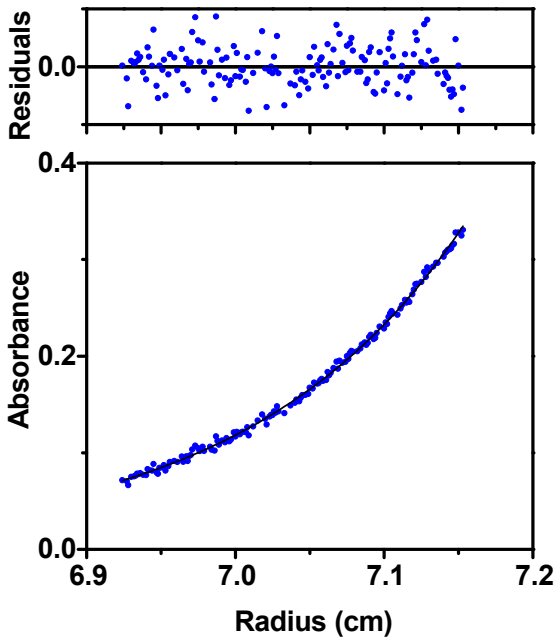

FIGURE 2-9: Sedimentation-equilibrium data for pTsr in the presence of 1 mM L-serine. The sample contained 8 μM pTsr. Data are shown as solid circles. The smooth curve represents a nonlinear fit to equation [2-3]. The residuals are shown in upper panel. The average molecular mass obtained was 32.5 ± 0.2 kDa.

Table 2-1: Molecular mass determination for pTsr using sedimentation-equilibrium.

pTsr Conc (μM)	Temp (°C)	[Ser] (mM)	Calcd MW (kDa)
8.4	4	0	20.60 ± 0.14
13.0	4	0	20.50 ± 0.17
13.8	25	0	21.40 ± 0.13
28.0	25	0	21.30 ± 0.11
29.2	4	0	21.50 ± 0.10
40.7	25	0	21.90 ± 0.06
41.1	4	0	21.60 ± 0.10
48.1	4	0	21.90 ± 0.07
3.3	4	10	30.50 ± 0.34
5.3	4	1	30.60 ± 0.44
8.4	4	1	32.50 ± 0.19
17.0	4	10	34.10 ± 0.12
17.0	4	1	32.60 ± 0.13
21.4	4	10	31.90 ± 0.27
32.9	4	10	31.50 ± 0.12
33.9	4	1	31.40 ± 0.11
36.0	4	10	31.40 ± 0.23
69.4	4	10	30.30 ± 0.12

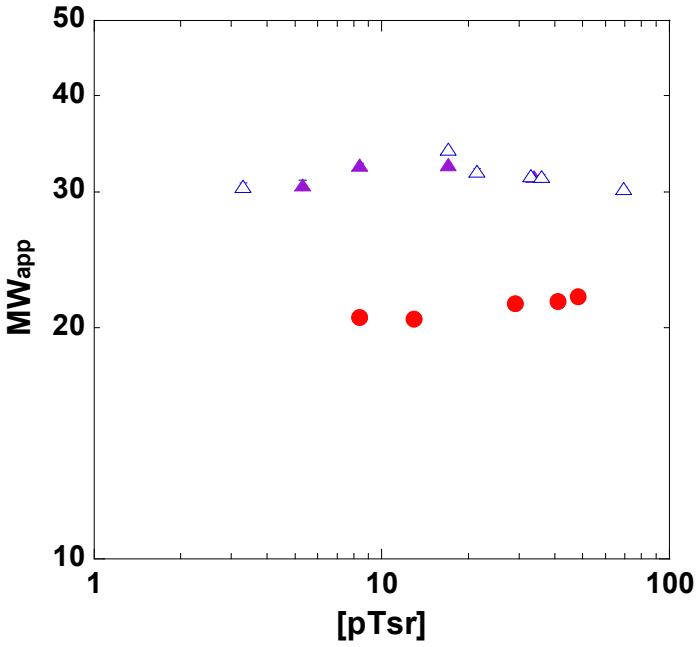

FIGURE 2-10: Apparent molecular mass of pTsr determined using sedimentation-equilibrium at 4°C. The apparent molecular mass was plotted as a function of pTsr concentration. Data are shown as solid circles, open triangles, and solid triangles representing samples containing 0 mM, 1 mM, and 10 mM L-serine, respectively.

as protein concentration increased, either in the absence or presence of L-serine. This result implies that neither the larger-than-monomer apparent molecular mass obtained in the absence of the ligand nor the smaller-than-dimer apparent molecular mass obtained in the presence of the ligand was due to the existence of both monomeric and dimeric species. Although they were not seen during the SDS-PAGE, there might be some contaminant proteins in the samples that caused the inaccurate values in the apparent molecular masses.

Conclusions

Both analytical gel-filtration and sedimentation-equilibrium indicate that pTsr exists mostly as a monomer in the absence of ligand and associates to form a dimer in the presence of L-serine. Increasing concentration of the ligand results in a higher apparent molecular mass. When a saturating concentration of the ligand is present, the dominant form of pTsr is a dimer. The intermediate apparent molecular masses obtained by analytical ultracentrifugation in the absence and presence of saturating concentrations of L-serine may be due to the presence of some contaminant that was not detected by SDS-PAGE in the protein preparation. The single sharp peaks resolved by gel-filtration chromatography together with the intermediate apparent molecular masses obtained in the presence of subsaturating concentrations of L-serine indicate that the species are in a rapid-exchange equilibrium. Taken together, the data most strongly argue that L-serine-binding induces dimerization of pTsr. A saturating concentration of L-leucine only

increases the apparent molecular mass of pTsr slightly, which may indicate a very weak binding.

According to the gel-filtration chromatography data, the dissociation constant for L-serine is in the range of 10 μM to 100 μM when the protein concentration is 5 μM. In principle, this estimate could be confirmed by analytical ultracentrifugation. However, our analytical ultracentrifugation data were obtained in the absence or presence of saturating concentrations of L-serine. More data obtained in the presence of intermediate concentrations of L-serine would be required to determine the monomer-dimer equilibrium constant as a function of L-serine concentration. From such data, the dissociation constant for L-serine with pTsr could be determined.

CHAPTER III

CHARACTERIZATION OF THE PERIPLASMIC DOMAIN OF TSR - LIGAND-BINDING (PART II)

Bacteria can sense concentration changes of L-serine, an attractant, and L-leucine, a repellent, through Tsr, a major chemoreceptor on the inner membrane of *E. coli* (Springer et al., 1977; Tso and Adler, 1974). In Chapter II, the oligomeric states of the periplasmic domain of Tsr (pTsr) was determined. It was found that pTsr exists mostly as a monomer in the absence of ligand and forms a dimer in the presence of L-serine. Unlike L-serine, saturating concentration of L-leucine induced only a small change in the apparent molecular mass. In this chapter, the ligand-binding properties of pTsr, including its binding stoichiometry and binding affinity, are characterized.

The biological functions of proteins are generally studied in terms of how they interact with other components in living systems. Proteins can interact with a large variety of ligands, which include other proteins, enzyme cofactors, metabolic intermediates, nucleic acids, nucleotides, amino acids and metal ions. The molecules that bind to proteins are defined as ligands. These interactions play critical roles in complex physiological processes, including oxygen transport, gene regulation, and immune responses. The characteristics of protein-ligand interactions allow an organism to respond quickly to metabolic and environmental changes. For these reasons, an understanding of protein-ligand interactions is essential to comprehend the function of biochemical systems.

Three aromatic amino acid residues in proteins (tyrosine, tryptophan, and phenylalanine) are responsible for the intrinsic fluorescence emission of proteins (Konev, 1967; Weinryb and Steiner, 1971; Demchenko, 1981; Permyakov, 1993). Tryptophan absorbs at the longest wavelength and displays the largest extinction coefficient. Energy transfer from phenylalanine and tyrosine to tryptophan in the same protein often occurs due to the long absorbing wavelength of tryptophan. When proteins are excited at 295-305 nm, the observed fluorescence is almost exclusively from tryptophan (Longworth, 1983). A valuable characteristic of tryptophan emission is that it is highly sensitive to the local environment of the tryptophan residue (Burstein et al., 1974). The association of a protein with other molecules often induces conformational changes and may consequently result in changes in the emission spectrum (Zukin, 1979). Steady-state fluorescence has been widely used to monitor protein-ligand interactions (Lakowicz, 1994; Callis, 1997). Binding parameters, such as the dissociation constant and binding stoichiometry, can be determined using this technique.

Steady-state fluorescence intensity is a measure of the total fluorescence emission from the fluorophores under excitation. The sample is excited with vertically polarized light, whose electric vector is orientated parallel to the vertical (z-axis). Emission is measured through an emission polarizer oriented either parallel (//) to the direction of the polarized excitation beam ($I_{//}$) or perpendicular ($\perp$) to the excitation beam ($I_{\perp}$). The total florescence emission (I_{tot}) is given by the following equation:

$$I_{tot} = I_{//} + 2I_{\perp} \qquad [3\text{-}1]$$

Materials and Methods

Materials. All chemical reagents and buffers were of analytical grade and were purchased from Fisher Scientific or Sigma-Aldrich. Sephadex G-100, a size exclusion resin, was obtained from Amersham Pharmacia Biotech. Mono Q10/10, an anion exchange column, was purchased from Amersham Pharmacia Biotech for use on their Fast Performance Liquid Chromatography (FPLC) system. BCA protein assay reagents were purchased from Pierce. BL21(DE3) *E. coli* cells that had been transformed with plasmid pGEM-3Z, which encodes the periplasmic domain of Tsr (pTsr32-188), was kindly provided by Dr. Michael D. Manson (Department of Biology, Texas A&M University).

EPPS buffer was spectral grade and purchased from Acros. L-serine and L-leucine was purchased from Sigma-Aldrich. L-serine and L-leucine solutions were prepared in 25 mM EPPS buffer and pH was adjusted to 7.4. Protein samples were stored in EPPS buffer at pH 7.4. Before fluorescence measurements were performed, all samples were filter sterilized through a Millipore PES Express 0.22 μM syringe-driven filter and incubated at room temperature for 30 min. Four-wall H-shaped quartz cuvettes were used, and the sample volume was 1 mL.

Protein Purification. The purification of pTsr was described in Chapter II. Some of the experiments performed to determine the K_d for L-serine, including all the L-leucine competition experiments, used pTsr obtained by Procedure I. The rest of the experiments used protein purified by Procedure II.

Steady-State Fluorescence. The total intensity of steady–state fluorescence was determined using an ISS Koala photo-counting spectrofluorometer. Intensity was attenuated using neutral density filters in the excitation path. The excitation wavelength was 300 nm. The excitation slit width was 0.5 mm, and the emission slit width was 1 mm. These dimensions correspond to bandwidths of 4 nm and 8 nm, respectively. Emission was measured through a Schott WG 345 nm cut-on filter. Data were collected until the relative error was less than 0.002. The temperature during the experiments was held at 25°C with a circulating water bath.

Data Analysis. Data were fit to appropriate equations using the non-linear least square fitting analysis of Kaleidagraph 3.5 software (Synergy). L-serine and L-leucine were used for characterizing ligand-binding properties of pTsr. The binding stoichiometry for L-serine binding to pTsr was determined using fluorescence spectroscopy. In principle, the total protein concentration should be much greater than the dissociation constant of ligand-binding. The fluorescence intensity of the sample was monitored as L-serine was added. The relative fluorescence intensity as a function of the molar ratio of total ligand to total protein concentration was plotted and fit to the following equation (Riley-Lovingshimer and Reinhart, 2005)

$$I = I_0 + \Delta I\left(\frac{\left(n + \frac{[A]_t}{[E]_t} + \frac{K_d}{[E]_t}\right) - \left[\left(n + \frac{[A]_t}{[E]_t} + \frac{K_d}{[E]_t}\right)^2 - 4n\frac{[A]_t}{[E]_t}\right]^{1/2}}{2n}\right) \qquad [3\text{-}3]$$

where I is the measured fluorescence intensity, I_0 is the initial total intensity, ΔI is the total change in intensity upon complete saturation, $[A]_t$ is total ligand concentration, $[E]_t$

is total protein concentration, K_d is the dissociation constant for the protein ligand complex (EA), and n is the binding stoichiometry. This model assumes that the ligand-binding affinities at all binding sites are equal and independent.

To determine ligand-binding affinities, steady-state fluorescence intensity was measured at an increasing concentration of each ligand. Measurements were also performed by varying concentrations of one ligand while the concentration of the other ligand was held constant. The total fluorescence intensity was corrected for dilution factors. Data were analyzed by plotting relative fluorescence intensity as a function of ligand concentration and fit to a modified version of the Hill equation (Hill, 1910).

$$F = \frac{\Delta F[A]^{n_H}}{K_d{}^{n_H} + [A]^{n_H}} + F0 \qquad [3\text{-}2]$$

where F is the relative steady-state fluorescence intensity, K_d is the concentration of ligand (A) that gives half-maximal fluorescence intensity, F_0 is equal to F when [A]=0, ΔF equals to the limiting value of $F\text{-}F_0$ when [A] is saturating, [A] is free ligand concentration and is assumed to equal the total ligand concentration under the condition that the protein concentration is much lower than the ligand-binding K_d, and n_H is the Hill coefficient. Different pTsr concentrations were used in the L-serine titration to test if protein concentration affects the measured dissociation constant for L-serine binding.

Results and Discussion

Stoichiometry. Based on the analytical gel filtration results described in Chapter II, the dissociation constant for L-serine at 5 μM pTsr is in the range of 10 μM to 100 μM. To establish stoichiometric conditions, 150 μM pTsr was used. Although we do not know for sure what the oligomeric state of the protein is at this concentration, according to the current knowledge of the dissociation constant for L-serine we can assume that the protein must be a dimer at the stoichiometry ligand concentration. An increase in the total fluorescence intensity was observed as L-serine was titrated into the pTsr solution (Figure 3-1). This result suggests that binding of L-serine causes a conformational change in pTsr and alters the local environment of either one or both tryptophan residues, W57 and W105, in pTsr. The L-serine binding stoichiometry (n) at 150 μM pTsr was found to be 0.5 bound L-serine molecules per pTsr monomer (solid line in Figure 3-1). The quality of the data fit was tested by fixing the value of n to 1 (dotted line) and 0.25 (dashed line), respectively. Panels A, B, and C in Figure 3-1 show the residuals of data fits when the value of n is not fixed, is fixed to 1, and is fixed to 0.25, respectively. Panel A shows the least structure, indicating the best data fit. The obtained stoichiometry is consistent with the value determined using wild-type Tsr on *E. coli* inner membrane (Lin et al., 1994), indicating that one molecule of L-serine is bound to a pTsr dimer at the experimental pTsr concentration.

L-Serine Binding. The dissociation constant (K_d) for L-serine was also determined by monitoring total fluorescence intensity while titrating L-serine into the pTsr solution (Figure 3-2). An inconsistency in the values of K_d determined using

A

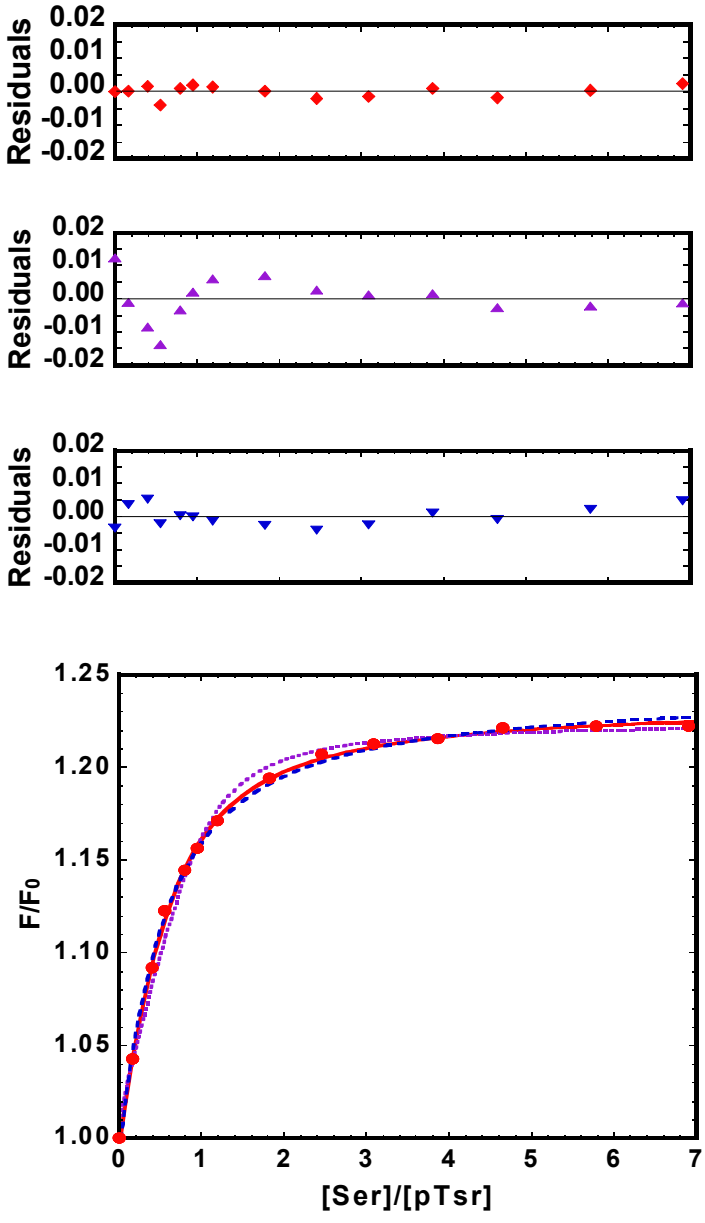

FIGURE 3-1: The stoichiometry of L-serine binding to 150 μM pTsr. The relative steady-state fluorescence intensity is plotted as a function of the molar ratio of L-serine to pTsr and is shown in the bottom panel. The solid circles represent experimental data points. The solid, dotted, and dashed lines represent the best fit to equation [3-3] when n is not fixed, n is fixed to 1, and n is fixed to 0.25, respectively. The corresponding residuals for the three fits are shown in panels A, B and C, respectively. The value determined for n is 0.5 L-serine per pTsr monomer.

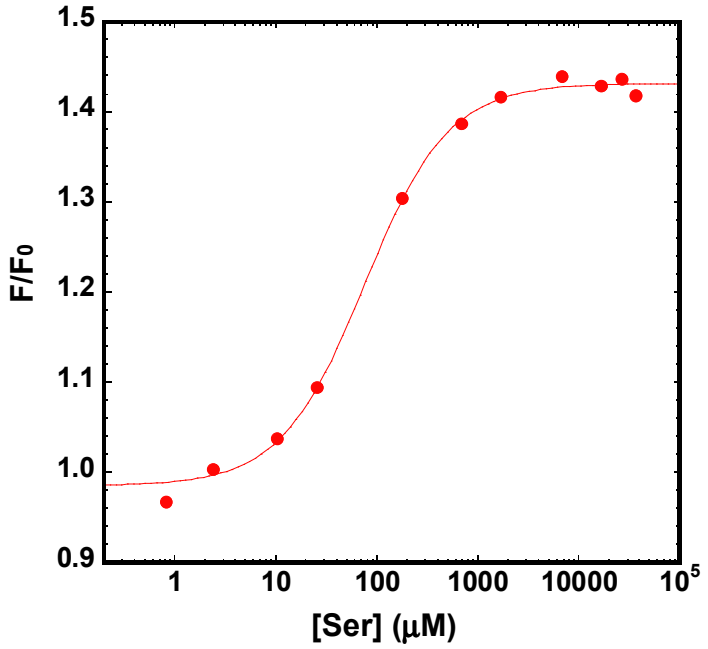

FIGURE 3-2: A representative plot of the effect of L-serine binding on the steady-state fluorescence intensity of pTsr purified using procedure I. The relative steady-state fluorescence intensity was plotted as a function of L-serine concentration. The pTsr concentration was 5 μM. The solid circles represent experimental data points, and the solid line represents the best fit to equation [3-2].

pTsr prepared by different purification procedures (Table 3-1) was noticed. The average value of the K_d for 5 μM pTsr purified by Procedure I, was 97 ± 8 μM. A much higher value for the K_d was obtained at 5 μM pTsr prepared by Procedure II. As the protein concentration increased, the K_d value became more similar to that determined using pTsr obtained by Procedure I. During Procedure II, the pH of the solution was adjusted to 6.0 for the second pass through the MonoQ column. It is possible that the low pH induced a change in protein conformation, for instance, by dissociating the pTsr dimer. Increased protein concentration may reverse this change.

Despite the inconsistency with pTsr from different purification procedures, an overall decrease in the L-serine binding K_d was observed as the initial pTsr concentration increased (Figure 3-3). This observation suggests that at higher protein concentrations, some properties of pTsr change to favor L-serine binding. Formation of homodimer has been shown with the periplasmic domain of aspartate receptor (Tar) at high protein concentrations and in the presence of aspartate (Daniel et al., 1993). Tar and Tsr are homologous proteins that share 34% sequence identity for periplasmic domain, it is possible that high protein concentration and ligand promote a shift in the monomer-dimer equilibrium of pTsr towards dimer. An additional condition is that ligand must bind to the dimer with higher binding affinity than to the monomer.

L-Leucine binding. When L-leucine was titrated into pTsr solution, no obvious change in the total fluorescence intensity was observed (Figure 3-4). It is possible that L-leucine binds to the same site as L-serine but does not elicit a fluorescence change

Table3-1: Dissociation constant determination for pTsr using fluorescence spectroscopy.

Prep	Purification Procedure	Date	[Tsr] (μM)	[Leu] (μM)	K_d (μM)	Stdv (μM)
1st	I	5/24/2004	0.5	0	600.2	86.2
1st	I	5/24/2004	1.0	0	459.5	96.3
1st	I	5/20/2004	2.5	0	153.4	19.8
1st	I	5/20/2004	5.0	0	75.3	8.0
1st	I	5/12/2004	5.0	0	76.4	4.8
1st	I	5/18/2004	5.0	0	96.7	7.6
1st	I	5/13/2004	5.0	0	104.0	9.8
1st	I	5/13/2004	5.0	0.5	102.6	6.6
1st	I	5/12/2004	5.0	500	76.5	4.4
1st	I	5/13/2004	5.0	1000	107.9	10.0
1st	I	5/13/2004	5.0	5000	112.6	7.1
1st	I	5/13/2004	5.0	8100	104.7	6.6
1st	I	5/20/2004	10.0	0	78.5	12.0
1st	I	5/20/2004	21.3	0	45.7	6.2
2nd	II	6/29/2004	0.6	0	330.4	61.7
2nd	II	6/29/2004	2.5	0	306.0	25.0
2nd	II	6/23/2004	5.0	0	94.0	5.3
2nd	II	6/29/2004	5.0	0	127.0	22.7
2nd	II	6/29/2004	9.1	0	155.4	93.6
3rd	II	9/10/2004	5.0	0	485.1	45.6
3rd	II	9/10/2004	23.0	0	63.0	3.1
3rd	II	9/10/2004	69.0	0	55.5	4.4
3rd	II	9/10/2004	115.0	0	88.3	17.4

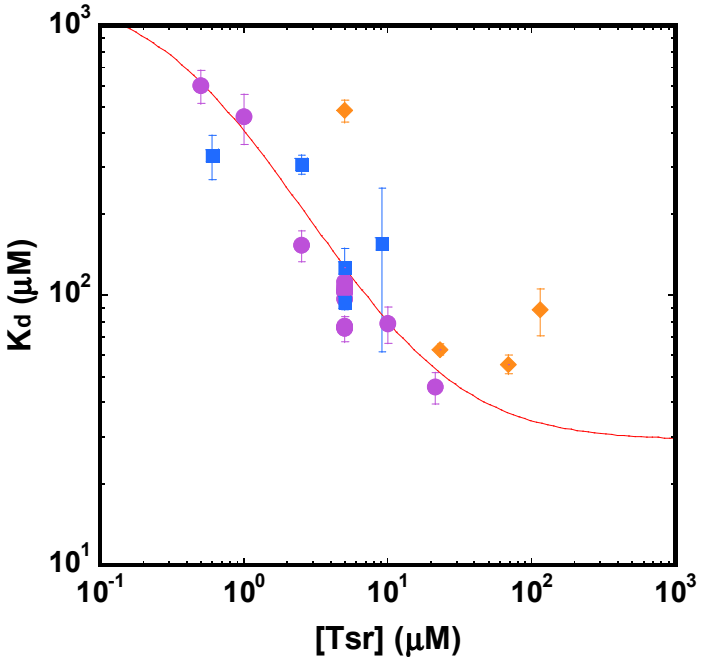

FIGURE 3-3: Effect of protein concentration on the apparent K_d for L-serine binding. The apparent dissociation constant for L-serine was plotted as a function of the pTsr concentration. The solid purple circles represent experimental data obtained pTsr that was purified by Procedure I. The solid blue squares represent experimental data obtained using pTsr that was purified by Procedure I. The solid orange diamonds represent experimental data obtained using a second pTsr prep purified by Procedure II. A inverse relationship between the protein concentration and the apparent dissociation constant is evident. The solid line represents the best fit to equation [3-12].

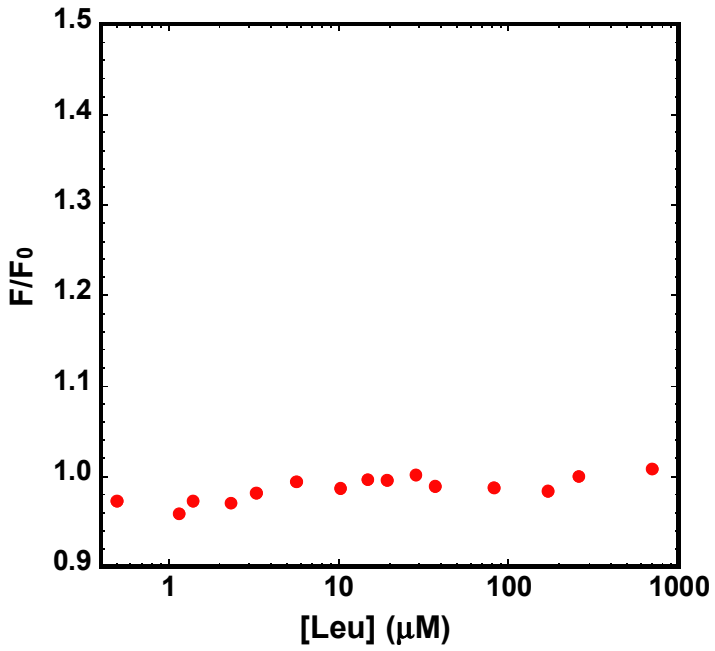

FIGURE 3-4: Effect of L-leucine on the steady-state fluorescence intensity of pTsr. The relative steady-state fluorescence intensity was plotted as a function of L-leucine concentration. The pTsr concentration was 5 μM. The solid circles represent experimental data points. The steady-state fluorescence intensity shows no significant change as L-leucine concentration increases.

upon binding. To address this possibility, competition experiments were performed. The apparent dissociation constant (K_d) for L-serine binding remained constant at various concentrations of L-leucine (Figure 3-5). There are several possible explanations for this observation. L-leucine may bind to a different, uncoupled binding site than L-serine, or L-leucine may bind to the same site but with a much lower binding affinity (the K_d must be greater than 100 μM) than L-serine. It is also possible that L-leucine does not bind at all to pTsr in these preparations.

Conclusions

A binding stoichiometry of 0.5 L-serine molecules bound per pTsr monomer was observed at a concentration of 150 μM pTsr indicating that one L-serine molecule binds per pTsr dimer.

The ligand-binding affinities were determined for pTsr purified by two similar methods, Procedure I and Procedure II. The purification protocol appears to affect the dissociation constant for L-serine binding to pTsr. Nevertheless, an overall decrease in the L-serine binding K_d as protein concentration increases was observed.

The characterization of ligand-binding properties of the periplasmic domain of Tsr only reveals the binding properties of L-serine. No binding of L-leucine was observed using fluorescence spectroscopy. In addition, L-leucine does not appear to compete for L-serine binding.

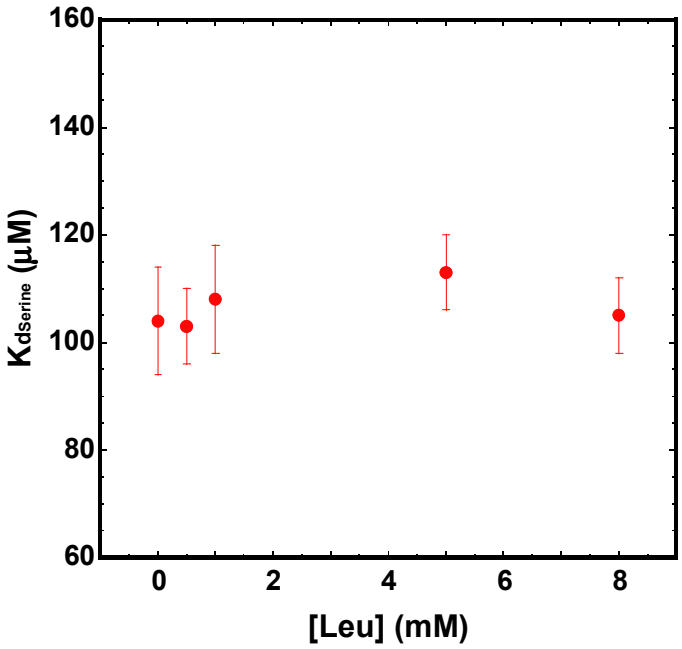

FIGURE 3-5: Effect of L-leucine concentration on the apparent L-serine binding K_d at 5µM. The apparent dissociation constant for L-serine was plotted as a function of L-leucine concentration. The solid circles represent experimental data points.

Based on the information collected for pTsr, a model can be proposed for the interaction between L-serine and pTsr (Figure 3-6). Dissociation constants for each binding event can be written as:

$$K_d = \frac{[M][M]}{[D]} \quad [3\text{-}4]$$

$$K_{d/a} = \frac{[M-Ser][M]}{[D-Ser]} \quad [3\text{-}5]$$

$$K_a = \frac{[M][Ser]}{[M-Ser]} \quad [3\text{-}6]$$

$$K_{a/d} = \frac{[D][Ser]}{[D-Ser]} \quad [3\text{-}7]$$

where [M] and [M-Ser] represent the concentration of the receptor monomer with no or one bound L-serine molecule and [D] and [D-Ser] represent the concentration of the receptor dimer with no and one bound L-serine molecule, respectively. K_d and $K_{d/a}$ are the dissociation constants for the pTsr monomer-dimer equilibrium when there is no and one bound L-serine molecule per pTsr dimer, and K_a and $K_{a/d}$ are the dissociation constants for L-serine binding to pTsr monomer and pTsr dimer.

The interactions between pTsr monomers and between pTsr monomers or dimers with L-serine can be quantified by a coupling constant Q:

$$Q = \frac{K_d}{K_{d/a}} = \frac{K_a}{K_{a/d}} \quad [3\text{-}8]$$

which represents the effect of L-serine binding to pTsr on the interaction between pTsr subunits or vice versa. Substituting equation [3-4] and [3-5] or equation [3-6] and [3-7] into equation [3-8] gives:

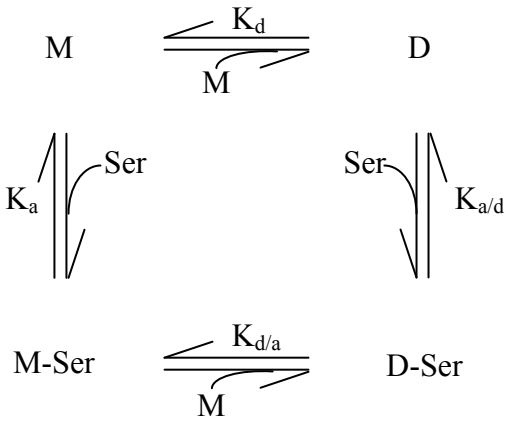

FIGURE 3-6: A simplified scheme depicting the interactions between L-serine and pTsr. M and D represent pTsr monomer and dimer. M-Ser and D-Ser represent pTsr monomer and dimer with a bound L-serine molecule. The respective dissociation constants are denoted by K with the appropriate subscript.

$$Q = \frac{[M][D-Ser]}{[M-Ser][D]} \qquad [3\text{-}9]$$

Therefore, Q also represents the thermodynamic equilibrium constant for the following equation:

$$M + D\text{-}Ser \underset{}{\overset{Q}{\rightleftharpoons}} M\text{-}Ser + D \qquad [3\text{-}10]$$

The dimerization of pTsr promotes L-serine binding when Q >1 and inhibits L-serine binding when Q <1. When Q =1, dimerization of pTsr does not affect L-serine binding.

The influence of dimerization on a measurable signal from (in our case F, the relative steady-state fluorescence intensity) pTsr can be described as in equation [5-10] if the substrate of pTsr is in rapid equilibrium (Reinhart, 1983; Reinhart, 1985):

$$F/[T] = \frac{F^0 K_d [Ser] + F^0 Q\, W [Ser][M]}{K_d [Ser] + K_a [M] + Q\, [Ser][M] + K_a K_d} \qquad [3\text{-}11]$$

where [T] is the total concentration of pTsr subunits in all forms, [Ser] is L-serine concentration, [M] is the concentration pTsr monomer, F^0 is the maximum relative steady-state fluorescence intensity when all pTsr molecules exist in monomer form, K_a is the dissociation constant of L-serine binding to pTsr monomer, K_d is the dissociation constant of the pTsr monomer-dimer equilibrium, Q is the ratio of the L-serine binding dissociation constants for L-serine binding to pTsr monomer and dimer, and W is the ratio of the maximum relative steady-state fluorescence intensity for pTsr in its dimeric and monomeric forms.

When W = 1 and F/[T] = $F^0/2$, solving for [Ser] gives:

$$K_a^{app} = K_a \left[\frac{K_d + [M]}{K_d + Q\, [M]}\right] \qquad [3\text{-}12]$$

where K_a^{app} is the apparent dissociation constant for L-serine binding to pTsr.

Fitting the data shown from Figure 3-3 to equation [3-12] gives K_d = 1.4 ± 0.5 mM, K_a = 19± 18 μM, and Q = 47± 30. Substituting the values into equation [3-8] gives $K_{d/a}$ = 30 ± 17 μM and $K_{a/d}$ = 0.4 ± 0.6 μM. Repeating the experiments using only protein purified by one procedure may decrease the error. Also, acquiring more data from analytical ultracentrifugation runs at non-saturating L-serine concentrations will help determine K values more accurately. Despite the imprecise K values currently available for pTsr, it is clear that our data are consistent with previous studies of the aspartate chemoreceptor (Tar) from *Salmonella typhimurium* (Milligan and Koshland, 1993). At low protein concentrations, the periplasmic domain of Tar was predominantly monomeric in the absence of aspartate. Addition of a saturating concentration of aspartate induced dimerization by increasing the monomer-monomer affinity at least 100 fold.

CHAPTER IV

CheA KINASE ACTIVITY ASSAYS

In the signal transduction pathway of bacterial chemotaxis, the histidine kinase CheA plays the key role catalyzing the phosphorylation of a response regulator, CheY. CheA is activated upon formation of a ternary complex with a coupling protein, CheW, and a chemoreceptor (Borkovich et al., 1989). Attractant binding to the Tsr chemoreceptor negatively regulates the kinase activity of CheA (Borkovich et al., 1989). CheY and ATP are both substrates for CheA. Kinetic assays showed that formation of the ternary complex increases the maximum activity of CheA and increases its affinity for ATP (Levit et al., 1999), indicating that a combination of V-type and K-type regulate CheA activity. In order to determine the effect of L-serine binding on the kinase-stimulating activity of Tsr, CheA activity in the ternary complex are assayed in the absence and presence of L-serine. Optimization of an alternative assay for measuring the CheA activity spectrophotometrically is also described in this chapter.

In the presence of ATP, CheA autophosphorylates and then transfers the phosphoryl group to CheY to form phosphor-CheY (CheY-P) (Stock et al., 1988; Hess et al., 1988a). The activity of CheA is measured by the rate of phosphorylation of CheY. One way to detect the reaction is to use radioactive phosphorylation assays:

$$[\gamma\text{-}^{32}\text{P}]\ \text{ATP} + \text{CheY} \xrightarrow{\text{CheA}} \text{ADP} + \text{CheY-}^{32}\text{P} \qquad [4\text{-}1]$$

The production of CheY-^{32}P can then be determined by autoradiography (Borkovich and Simon, 1991). End-point assays can be performed at different time points, and the reaction rate can be calculated from the slope of the linear portion of a plot of CheY-^{32}P production as a function of time.

The radioactive assay uses a single time point to determine the turnover rate of CheA. Therefore, control of the reaction time is critical. In addition, the observation of the reaction is not in real time, a circumstance that limits the types of measurements that can be made. The inconvenience of using ^{32}P is another drawback. In order to solve these problems, a potentially more versatile assay is being designed and optimized based on a previously described method (Norby, 1988; Ninfa *et al.*, 1991). Spectrophotometric assays of CheA activity take advantage of the spectroscopic characteristics of NADH. Figure 4-1 describes the phosphorylation of CheY by CheA coupled to reactions catalyzed by pyruvate kinase and lactate dehydrogenase. The production of CheY-P is therefore indirectly coupled to the oxidation of NADH, which can be detected by a decrease in absorbance of NADH at 340 nm as a function of time.

Materials and Methods

Materials. All chemical reagents and buffers were of analytical grade and purchased from Fisher Scientific or Sigma-Aldrich. The sodium salt of ATP and dithiothreitol were purchased from Roche Diagnostics. NADH and the potassium salt of ADP were purchased from Sigma. Membranes from cells overproducing Tsr, and

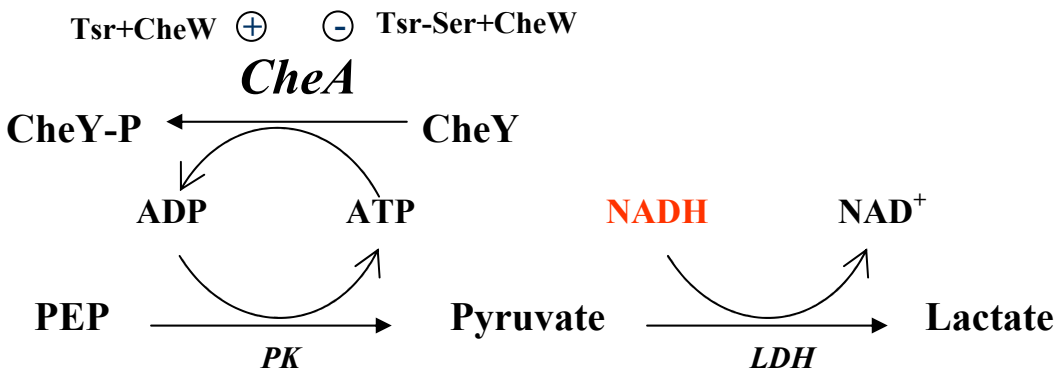

FIGURE 4-1: Schematic representation of a coupled assay for CheA activity. CheA activity is measured by monitoring oxidation of NADH. Enzymes are shown in italics. PEP is phopho(enol)pyruvate, PK is pyruvate kinase, LDH is lactate dehydrogenase, NADH is nicotinamide adenine dinucleotide (reduced form), and NAD^+ is nicotinamide adenine dinucleotide (oxidized form).

purified CheW, CheA and CheY were kindly provided by Dr. Michael D. Manson (Department of Biology, Texas A&M University).

Radioactive Phosphorylation Assays. To determine the effects of ligand-binding on CheA kinase activity, radioactive phosphorylation assays were performed according to Borkovich and Simon (1991), with modifications. Five pmol CheA and 20 pmol CheW were mixed and incubated on ice overnight. Then 20 pmol membrane-bound Tsr (30-50 percent of total membrane protein), and 500 pmol of CheY were added to the CheA/CheW mix in a total volume of 8 µl of fresh phosphorylation buffer (50mM Tris-HCl [pH 7.5], 50 mM KCl, 5 mM $MgCl_2$, and 2 mM DTT). One µl of 2.6 mM solution of L-serine or ddH_20 was added to each tube. The mixture was incubated for 4 h at room temperature to allow the assembly of ternary complexes. The phosphorylation reactions were initiated by adding 1 µl of [γ-^{32}P] ATP (3000 Ci/mmol NEN# BLU502A) and 1 µl of a solution with the desired concentration of unlabeled ATP. It has previously been shown that CheY-P production in this reaction mixture has a linear relationship with time for at least 20 s when the final ATP concentration is 500 µM for the reaction mixture (Draheim et al., 2005). The activity of the enzyme can be calculated based on the amount of CheY-^{32}P produced over 20 s. Although the reaction might not be linear at all ATP concentrations, we used the 20-s stopping point in the assays because of the limited supply of materials. The reactions were stopped by addition of 40 µl 2x SDS-PAGE loading buffer containing 25 mM of EDTA. Samples were then subjected to 17% SDS-PAGE. Gels were dried and autoradiographed. CheY-^{32}P production was quantified by densitometry. A series of [γ-^{32}P] ATP dilution spots were used for calibration of [^{32}P].

Reaction rates (v) were determined at different ATP concentrations. The reaction rates were then plotted as a function of ATP concentrations, and the data were fit to the Michaelis-Menton equation:

$$v = \frac{V_{\max}[A]}{K_m + [A]} \qquad [4\text{-}5]$$

where v is the reaction velocity, V_{max} is the maximum reaction velocity, [A] is the ligand concentration, and K_m is the concentration of ligand (A) that gives half-maximal activity. The same reactions were carried out in the presence 260 μM L-serine, and the K_m and V_{max} values determined in the presence and absence of the L-serine were compared.

Spectrophotometric Assays of CheA Activity. This method is still in the process of being optimized. The rate of phosphorylation of CheY can be determined spectrophotometrically using a pyruvate kinase/lactate dehydrogenase coupled enzyme system (Norby, 1988; Ninfa, *et al.*, 1991). In the first experiments, 50 pmol CheA and 200 pmol CheW were mixed and incubated on ice overnight. Then, 200 pmol membrane-bound Tsr was added to the CheA/CheW mix in a total volume of 10 μL. This mixture was incubated for 4 h at room temperature to allow assembly of functional ternary complexes. Reactions were carried out at 35 C° in reaction buffer (0.1 mM dithiothreitol, 100 mM potassium phosphate [pH7.5], and 5 mM magnesium chloride). Reactions were initiated by addition of 1 μL of the protein mixture into a total volume of 99 μL of reaction buffer containing 0.80 mM NADH, 3 mM ATP, 1.0 mM phosphoenopyruvate, 4 units of pyruvate kinase, 4 units of lactate dehydrogenase, and 50 μM CheY. The rate of NADH oxidation was measured by monitoring the decrease of

absorbance at 340 nm as a function of time, using a Beckman DU-640 spectrophotometer.

Results and Discussion

Radioactive Phosphorylation Assays. The results obtained from the radioactive phosphorylation assays showed that there was an approximately 70% decrease in the activity at the highest ATP concentration used (3 mM) upon addition of 260 μM L-serine (Figure 4-2). A K_m value of 632 ± 82 μM for ATP concentration was determined in the absence of L-serine. With 260 μM L-serine present, the K_m value was 716 ± 50 μM. These preliminary data suggest that the inhibitory effect of L-serine on the CheA kinase-stimulating activity of Tsr is of the V-type rather than K-type for the substrate ATP. However, more complete study using a range of L-serine concentrations should be performed before final conclusion can be made.

Spectrophotometric Assays of CheA Activity. In developing this assay, the first step was adapting the method to conduct the assay in a small volume. The total volume of an enzyme assay monitored with a Beckman DU-640 spectrophotometer is often as large as 1 mL. The receptor-coupled CheA-activity assay requires the use of multiple purified proteins. To minimize the consumption of proteins, we decreased the reaction volume to 100 μL by using 3 x 3 mm fluorescence cuvettes and the corresponding cuvette holders. A 5 μL micro-syringe was used to facilitate accurate measurement of reaction components, and an end-sealed microcapillary was used to mix the reaction components before starting to monitor the reaction.

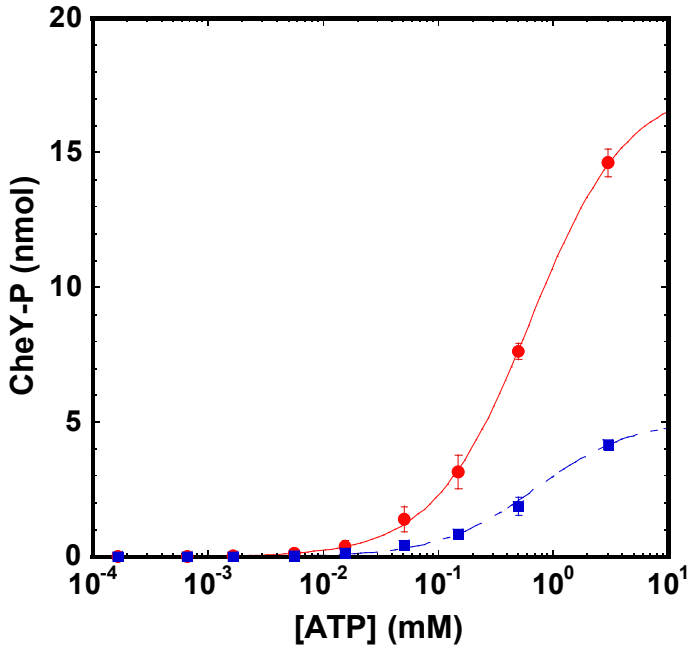

FIGURE 4-2: ATP dependence of Tsr coupled CheA activity. The data obtained in the absence and presence of 260 μM L-serine are shown as solid circles and solid squares, respectively. The solid lines represent the fit of the data to equation [4-5].

Chemoreceptors are normally embedded in the cell membrane. In order to measure the activity of Tsr under these conditions, we used inner-membrane preparations enriched for *E. coli* Tsr. The enzymatic complexity of the *E. coli* inner membrane provides challenges to the application of the enzyme-coupled assay. Resident NADH dehydrogenase, NADH oxidase, and ATPase present in the membranes either directly or indirectly consume NADH (Ingledew and Poole, 1984). The consumption of NADH by these reactions does not require CheA, so that the reaction rate measured in this assay includes a background rate generated by these enzymes. This situation is further complicated by the inhibitory effect of ADP and ATP on NADH dehydrogenase activities (Dancey and Shapiro, 1976). The high background reaction rate can be corrected for by running a separate reaction in the absence of CheY, the CheA substrate. The net rate of CheY-P production can then be obtained by subtracting the background rate from the total reaction rate. However, the reproducibility of the assay has been an issue due to the background rate that is higher than the CheA-dependent reaction rate.

To optimize the reaction conditions and maximize the ratio of the CheA-dependent reaction rate to the background rate, reactions were run at various temperatures. The ratio of the two rates were plotted against temperature (Figure 4-3). An overall trend of higher temperature producing a higher ratio was observed.

The reliability of the assay was tested by determining the CheA-dependent reaction rates at various CheY concentrations (Figure 4-4). The rate increased with CheY concentration. Fitting the data to equation [4-5] gave a K_m value of 40 ± 10 μM for CheY binding to CheA. Purified CheA has been shown to bind CheY with a

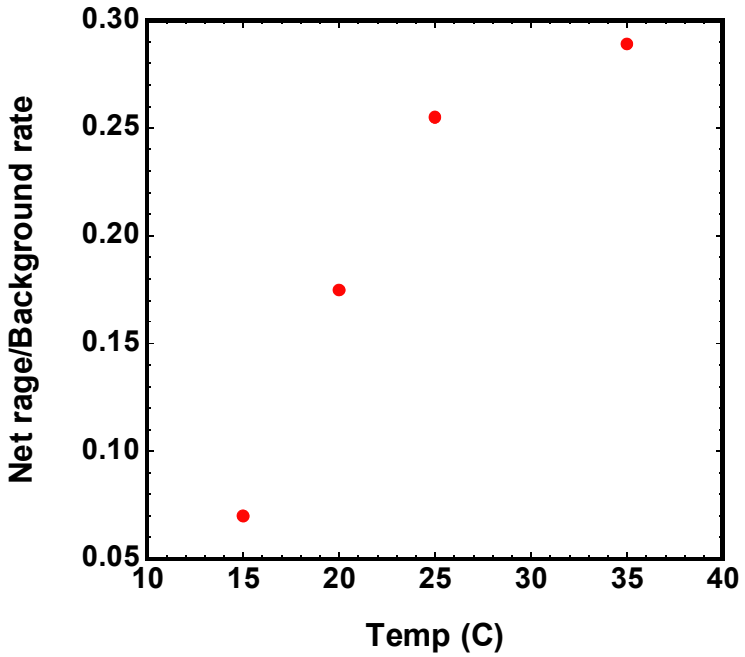

FIGURE 4-3: Spectrophotometric assay of the CheA-dependent (net) activity - temperature dependence of the ratio of reaction rate to the background reaction rate. The solid circles represent reaction rates.

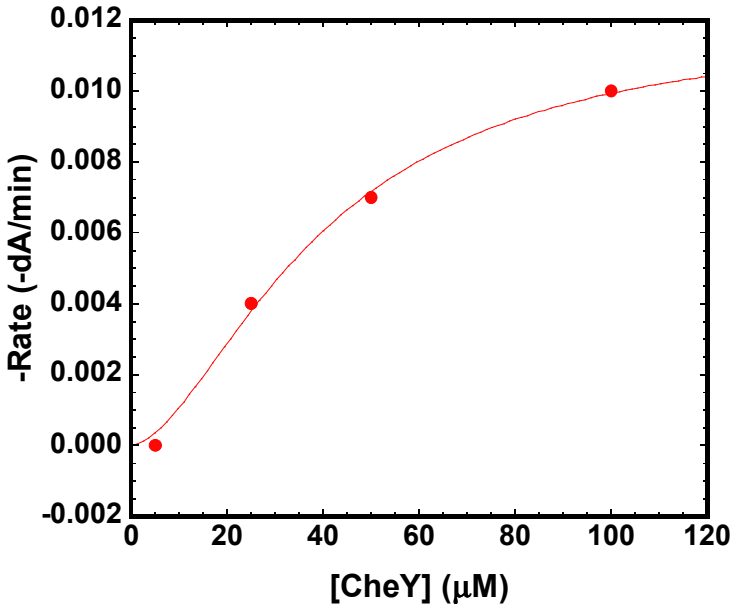

FIGURE 4-4: Spectrophotometric assay of CheA activity as a function of CheY concentration. The solid circles represent the reaction rates determined at various CheY concentrations. The solid line represents the fit of the data to equation [4-5]. The K_m obtained for CheY binding to CheA is 40 ± 10 μM.

dissociation constant of 2.0 μM at 25°C (Li et al., 1995). A similar test was performed by recording reaction rates at different CheA concentrations (Figure 4-5). An increase in rate with increasing CheA concentration was observed. A proportional increase in the reaction rate to the increase in CheA concentration, which is expected in enzyme reactions, was observed when the rate was corrected to zero in the absence of the enzyme. Although the initial results with the assay were promising, there is still a long way to go before reliable results can be achieved.

The background rate may be decreased by lowering the amount of receptor-containing membrane while maintaining the same ratio of Tsr: CheW: CheA. However, the stability of the ternary complex at lower protein concentrations needs to be examined. The protein composition of the ternary complex can be estimated by the method of Mikhail et al. (1999). If the stability of the complex becomes a problem, optimization of the concentrations of the various components of the reaction will also be required.

Conclusions

The allosteric effects of L-serine on Tsr-coupled CheA activity were studied using a radioactive phosphorylation assay. The results showed that L-serine inhibited the activity of CheA without affecting the binding affinity of CheA for ATP. CheA kinase activity was also determined by a spectrophotometric assay. This assay monitors the phosphorylation of CheY by CheA to the oxidation of NADH by coupling the regeneration of ATP by pyruvate kinase to NADH oxidation by lactate dehydrogenase.

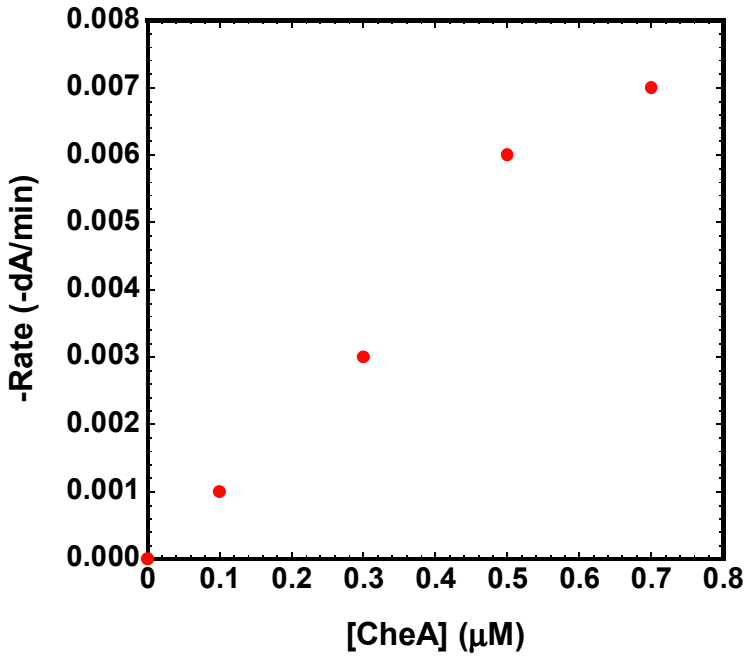

FIGURE 4-5: Spectrophotometric assay of CheA activity as a function of CheA concentration. The solid circles represent reaction rates determined at various CheA concentrations.

However, the high background rates found in the first tests show that considerable optimization of the assay is required.

CHAPTER V

CONCLUSIONS

Extensive structural, genetic and biochemical studies have been used to study the signal transduction pathways of *E. coli* chemotaxis (Bren and Eisenbach, 2000; Bourret and Stock, 2002). The complexes formed between chemoreceptors and the CheA histidine kinase, which also involve the coupling protein CheW, show the regulatory characteristics of allosteric proteins. However, little is known about the mechanism of allosteric regulation. The application of the current advanced understanding of allostery in soluble enzymes to the receptor/CheW/CheA ternary complex may shed light on the mechanism of transmembrane signaling that occurs as the initial step in chemotaxis.

The research described in this thesis was designed to characterize the ligand-binding properties of the periplasmic domain of the transmembrane serine chemoreceptor Tsr. This information was then extended to study how this regulatory domain controls the activity of the ternary complex of Tsr, CheW and CheA.

Chapter II focuses on the purification of the periplasmic domain of Tsr (pTsr) and the determination of its oligomeric states in the presence and absence of ligands. The methods employed were analytical gel-filtration and sedimentation-equilibrium ultracentrifugation. The results strongly suggest that L-serine induces dimerization of pTsr. In contrast, the repellent ligand L-leucine had little, if any, effect on dimerization. Analytical gel-filtration provided a dissociation constant (K_d) for L-serine between 10

μM and 100 μM when the concentration of pTsr monomer was 5 μM. To determine the K_d for L-serine more precisely, additional experiments could be performed using a range of L-serine concentrations between 10 μM and 100 μM.

Chapter III describes the determination of the ligand-binding properties of pTsr using steady-state fluorescence measurements. A stoichiometry of 0.5 bound L-serine molecules per pTsr monomer was obtained at a pTsr concentration of 150 μM. The K_d for L-serine binding was determined using this method and revealed that the value depends on protein concentration. However, no evidence for binding of L-leucine to pTsr was obtained, a result consistent with the findings from analytical centrifugation.

Combining the information from Chapter II and Chapter III, a working model was proposed for the interactions between L-serine and pTsr. The model accounts both for the effect of L-serine on the monomer-dimer equilibrium of pTsr and the effect of protein concentration on ligand-binding affinity. Values for the dissociation constants applicable to each binding event could be incorporated into the model.

A preliminary study of the coupling between L-serine binding to full-length, membrane-bound Tsr and the receptor-coupled kinase activity of CheA is described in Chapter IV. By using a modified version of a radioactive phosphorylation assay (Borkovich and Simon, 1991), my results indicate that L-serine exerts V-type inhibition on CheA activity rather than K-type inhibition, which would have revealed itself as an increase in the Km for ATP. In this chapter, preliminary steps in the optimization of an alternative method for measuring CheA activity are also reported. This assay monitors

the steady-state activity of CheA using the spectroscopic pyruvate kinase/lactate dehydrogenase coupled assay, first reported by Surette et al. (1996).

A number of questions remain about allosteric regulation in chemoreceptor complexes. For instance, how does binding of L-serine to Tsr affect its affinity for CheA, CheW, and CheY? How does L-leucine interact with Tsr to exert its effect as a repellent? What is the role of CheW in the regulation of the CheA activity? Which residues are important contributors to the communication between the allosteric site in the periplasmic domain and the active site of the kinase?

In summary, the periplasmic domain of Tsr was purified and its ligand-binding and dimerization properties were characterized. L-serine was shown to exert V-type inhibition on Tsr-coupled CheA activity. Finally, the development of an alternative assay for the steady-state activity of CheA was initiated. This assay, once optimized, will be much better suited to kinetic studies of the receptor-kinase complex than the radioactive assay currently in widespread use.

REFERENCES

Adler, J. 1969. Chemotaxis in bacteria. *Science.* 166, 1588-1579.

Adler, J., G. L. Hazelbauer, and M. M. Dahl. 1973. Chemotaxis toward sugars in *Escherichia coli. J. Bacteriol.* 115:824-847.

Ames, P. and J. S. Parkinson. 1994. Constitutively signaling fragments of Tsr, the *Escherichia coli.* serine chemoreceptor. *J. Bacteriol.* 176(20):6340-6348.

Basu, A., M. Raghunath, S. Bishayee, and M. Das. 1989. Inhibition of tyrosine kinase activity of the epidermal growth factor (EGF) receptor by a truncated receptor form that binds to EGF: role for interreceptor interaction in kinase regulation. *Mol. Cell. Biolo.* 9:671-677.

Berg, H. C. 1975. Bacterial behaviour. *Nature.* 254(5499):389-392.

Berg, H. C. and D. A. Brown. 1972. Chemotaxis in *Escherichia coli* analyzed by three-dimensional tracking. *Nature.* 239:500-504.

Berg, H. C. and D. A. Brown. 1974. Chemotaxis in *Escherichia coli* analyzed by three-dimensional tracking. *Antibiotics and Chemotherapy.* 19:55-78.

Berg, H. C. and P. M. Tedesco. 1975. Transient response to chemotactic stimuli in *Escherichia coli*. *Proc. Natl. Acad. Sci. USA*. 72:3235-3239.

Bibikov, S. I., R. Biran, K. E. Rudd, and J. S. Parkinson. 1997. A signal transducer for aerotaxis in *Escherichia coli. J. Bacteriol.* 179: 4075-4079.

Biemann, H. P. and D. E. Koshland Jr. 1994. Aspartate receptors of *Escherichia coli* and *Salmonella typhimurium* bind ligand with negative and half-of-the-sites cooperativity. *Biochemistry.* 33(3):629-634.

Borkovich, K. A., N. Kaplan, J. F. Hess, and M. I. Simon. 1989. Transmembrane signal transduction in bacterial chemotaxis involves ligand-dependent activation of phosphate group transfer. *Proc. Natl. Acad. Sci. USA.* 86:1208–1212.

Borkovich, K. A. and M. I. Simon. 1990. The dynamics of protein phosphorylation in bacterial chemotaxis. *Cell.* 63:1339-1348.

Borkovich, K. A. and M. I. Simon. 1991. Coupling of receptor function to phosphate-transfer reactions in bacterial chemotaxis, *Methods Enzymol.* 200:205-214.

Bornhorst, J. A. and J. J. Falke. 2000. Attractant regulation of the aspartate receptor-kinase complex: limited cooperative interactions between receptors and effects of receptor modification state. *Biochemistry.* 39:9486-9493.

Bourret, R. B. and A. M. Stock. 2002. Molecular information processing: lessons from bacterial chemotaxis. *J. Biol. Chem.* 277:9625-9628.

Bray, D. 2002. Bacterial chemotaxis and the question of gain. *Proc. Natl. Acad. Sci. USA*. 99:7-9.

Bray, D. and T. Duke. 2004. Conformational spread: The propagation of allosteric states in large multiprotein complexes. *Annu. Rev. Biophys. Biomol. Struct.* 33:53-73.

Bray, D., M. D. Levin, and C. J. Morton-Firth. 1998. Receptor clustering as a cellular mechanism to control sensitivity. *Nature.* 393:85-88.

Bren, A. and M. Eisenbach. 2000. How signals are heard during bacterial chemotaxis: protein-protein interactions in sensory signal propagation. *J. Bacteriol.* 182:6865-6873.

Brown, D. A. and H. C. Berg. 1974. Temporal stimulation of chemotaxis in *Escherichia coli*. *Proc. Natl. Acad. Sci. U S A.* 71(4):1388-92.

Burstein, E. A., N. S. Vedenkina, and M. N. Ivkova. 1974. Fluorescence and the location of tryptophan residues in protein molecules, *Photochem. Photobiol.* 18:263-279.

Callis, P. R. 1997. 1La and 1Lb transitions of tryptophan: applications of theory and experimental observations to fluorescence of proteins. *Methods Enzymol.* 278:113-150.

Clarke, S. and D. E. Koshland Jr. 1979. Membrane receptors for aspartate and serine in bacterial chemotaxis. *J. Biol. Chem.* 254(19):9695-9702.

Cluzel, P., M. Surette, and S. Leibler. 2000. An ultrasensitive bacterial motor revealed by monitoring signaling proteins in single cells. *Science.* 287:1652-1655.

Dancey, G. F. and B. M. Shapiro. 1976. The NADH dehydrogenase of the respiratory chain of *Escherichia coli. J. Biol. Chem.* 251(19):5921-5928.

Daniel, L. 1993. Purification and characterization of the periplasmic domain of the aspartate chemoreceptor. *J. Biol. Chem.* 268(27):19991-19997.

Demchenko, A. P. 1981. Ultraviolet Spectroscopy of Proteins, Springer-Verlag, New York.

Dower, S. K., J. M. Wignall, K. Schooley, C. J. McMahan, J. L. Jackson, K. S. Prickett, S. Lupton, D. Cosman, and J. E. Sims. 1989. Retention of ligand binding activity by the extracellular domain of the IL-1 receptor. *J. Immunol.* 142:4314-4320.

Draheim, R. R., A. F. Bormans, R. Z. Lai, and M. D. Manson. 2005. Tryptophan residues flanking the second transmembrane helix (TM2) set the signaling state of the Tar chemoreceptor. *Biochemistry.* 44:1268-1277.

Duan, D., M. J. Pazin, L. J. Fretto, and L. T. Williams. 1991. A functional soluble extracellular region of the platelet-derived growth factor (PDGF) beta-receptor antagonizes PDGF-stimulated responses. *J. Biol. Chem.* 266:413-418.

Falke, J. J. and G. L. Hazelbauer. 2001. Transmembrane signaling in bacterial chemoreceptors. *TRENDS in Biochemical Sciences.* 26:257-265.

Feng, X., A. A. Lilly, and G. L. Hazelbauer. 1999. Enhanced function conferred on low-abundance chemoreceptor Trg by a methyltransferase-docking site. *J. Bacteriol.* 181:3164-3171.

Foster, D. L., S. L. Mowbray, B. K. Jap, and D. E. Koshland Jr. 1985. Purification and characterization of the aspartate chemoreceptor. *J. Biol. Chem.* 260, 11706-11710.

Frieden, C. 1964. Treatment of enyme kinetic data. I. The effect of modifiers on the kinetic parameters of single substrate enzymes. *J. Biol. Chem.* 239:3522-3531.

Gegner, J. A., D. R. Graham, A. F. Roth, and F. W. Dahlquist. 1992. Assembly of an MCP receptor, CheW, and kinase CheA complex in the bacterial chemotaxis signal transduction pathway. *Cell.* 70(6):975-982.

Gestwicki, J. R. and L. L. Kiessling. 2001. Inter-receptor communication through arrays of bacterial chemoreceptors. *Nature.* 415:81-84.

Goy, M. F., M. S. Springer, and J. Adler. 1977. Sensory transduction in *Escherichia coli*: role of a protein methylation reaction in sensory adaptation. *Proc. Natl. Acad. Sci. USA* 74:4964-4968.

Gupta V., C. B. Peterson, L. T. Dice, T. Uchiki, J. Racca, J. T. Guo, Y. Xu, R. Hettich, X. Zhao, R. Rothstein, and C. G. Dealwis. 2004. Sml1p is a dimer in solution: characterization of denaturation and renaturation of recombinant Sml1p. *Biochemistry.* 43(26):8568-8578.

Harkness, D. R. 1971. The regulation of hemoglobin oxygenation. *Adv. Intern. Med.* 17:189-214.

Hazelbauer, G. L., C. Park, and D. M. Nowlin. 1989. Adaptational "crosstalk" and the crucial role of methylation in chemotactic migration by *Escherichia coli. Proc. Natl. Acad. Sci. USA*. 86:1448-1452.

Hess, J. F., R. B. Bourret, and M. I. Simon. 1988b. Histidine phosphorylation and phosphoryl group transfer in bacterial chemotaxis. *Nature.* 336(6195):139-143.

Hess, J. F., K. Oosawa, N. Kaplan, and M. I. Simon. 1988a. Phosphorylation of three proteins in the signaling pathway of bacterial chemotaxis. *Cell.* 53(1):79-87.

Hill, A. V. 1910. The possible effects of the aggregation of the molecules of hemoglobin on its dissociation curves. *J. Physiol.* 40:iv-vii.

Ingledew, W. J. and R. K. Poole. 1984. The respiratory chains of *Escherichia coli. Microbiol. Rev.* 48(3):222-271.

Jin, T. and M. Inouye. 1993. Ligand binding to the receptor domain regulates the ratio of kinase to phosphatase activities of the signaling domain of the hybrid *Escherichia coli* transmembrane receptor, Taz1. *J. Mol. Biol.* 232:484-492.

Kehry, M. R., T. G. Doak, and F. W. Dahlquist. 1984. Stimulus induced changes in methyleserase activity during chemotaxis in *Escherichia coli. J. Biol. Chem.* 259:11828-11835.

Kim, K. K., H. Yokota, and S. H. Kim. 1999. Four-helical-bundle structure of the cytoplasmic domain of a serine chemotaxis receptor. *Nature.* 400:787-792.

Koman, A., S. Harayama, and G. L. Hazelbauer. 1979. Relation of chemotactic response to the amount of receptor: evidence for different efficiencies of signal transduction. *J. Bacteriol.* 138:739-747.

Konev, S. V. 1967. Fluorescence and Phosphorescence of Proteins and Nucleic Acids, Plenum Press, New York.

Koshland, D. E., G. Nemethy, and D. Filmer. 1966. Comparison of experimental binding data and theoretical models in proteins containing subunits. *Biochemistry.* 5:365-385.

Laemmli, U. K. 1970. Cleavage of structural proteins during the assembly of the head of bacteriophage T4. *Nature.* 227:680-685.

Lai, R. Z., J. M. Manson, A. F. Bormans, R. R. Draheim, N. T. Nguyen, and M. D. Manson. 2005. Cooperative signaling among bacterial chemoreceptors. *Biochemistry.* 44:14298-14307.

Lakokwicz, J. R., I. Gryczynski, G. Laczko, W. Wiczk, and M. L. Johnson. 1994. Distribution of distances between the tryptophan and the N-terminal residue of melittin in its complex with calmodulin, troponin C, and phospholipids, *Protein Sci.* 3:628-637.

Levit, M. N., Y. Liu, and J. B. Stock. 1999. Mechanism of CheA protein kinase activation in receptor signaling complexes. *Biochemistry.* 38:6651-6658.

Li, G. Y. and R. M. Weis. 2000. Covalent modification regulates ligand binding to receptor complexes in the chemosensory system of *E. coli. Cell.* 100:357-365.

Li, J., G. Li, and R. Weis. 1997. The serine chemoreceptor from Escherichia coli is methylated through an inter-dimer process. *Biochemistry.* 36:11851-11857.

Lin, L. N., J. Li, J. F. Brandts, and R. M. Weis. 1994. The serine receptor of bacterial chemotaxis exhibits half-site saturation for serine binding. *Biochemistry.* 33(21):6564-6570.

Liu, Y., M. Levit, R. Lurz, M. G. Surette, and J. B. Stock. 1997. Receptor-mediated protein kinase activation and the mechanism of transmembrane signaling in bacterial chemotaxis. *EMBO J.* 16:7231-7274.

Longworth, J. W. 1983. Intrinsic fluorescence of proteins. Time-Resolved Fluorescence Spectroscopy in Biochemistry and Biology, R. B. Cundall and R. E. Dale (eds), Plenum Press, New York, 651-778.

Lupas, A. and J. Stock. 1989. Phosphorylation of an N-terminal regulatory domain activates the CheB methylesterase in bacterial chemotaxis. *J. Biol. Chem.* 264:17337-17342.

Macnab, R. M. and D. E. Koshland Jr. 1972. The gradient-sensing mechanism in bacterial chemotaxis. *Proc. Natl. Acad. Sci. USA.* 69:2509-2512.

Maddock, J. R. and L. Shapiro. 1993. Polar location of the chemoreceptor complex in the *E. coli* cell. *Science.* 259:1717-1723.

Maeda, K., Y. Imae, J. I. Shioi, and F. Oosawa. 1976. Effect of temperature on motility and chemotaxis of *Escherichia coli. J. Bacteriol.* 127:1039-1046.

Manson, M. D., V. Blank, G. Brade, and C. F. Higgins. 1986. Peptide chemotaxis in *E. coli* involves the Tap signal transducer and the dipeptide permease. *Nature.* 321:253-256.

Mao, H., P. S. Cremer, and M. D. Manson. 2003. A sensitive, versatile microfluidic assay for bacterial chemotaxis. *Proc. Natl. Acad. Sci. USA.* 100(9):5449-5454.

Mesibov, R. and J. Adler. 1972. Chemotaxis toward amino acids in *Escherichia coli. J. Bacteriol.* 112:315-326.

Milligan, D. L. and D. E. Koshland Jr. 1988. Site-directed cross-linking. Establishing the dimeric structure of the aspartate receptor of bacterial chemotaxis. *J. Biol. Chem.* 263(13):6268-6275.

Milligan, D. L. and D. E. Koshland Jr. 1993. Purification and characterization of the periplasmic domain of the aspartate chemoreceptor. *J. Biol. Chem.* 268(27):19991-19997.

Monod, J., J. Wyman, and J. P. Changeux. 1965. On the nature of allosteric transitions: a plausible model. *J. Mol. Biol.* 12:88-118.

Ninfa, E. G., A. Stock, S. Mowbray, and J. Stock. 1991. Reconstitution of the bacterial chemotaxis signal transduction system from purified components. *J. Biol. Chem.* 266:9764–9770.

Pace, N. C. 1995. How to measure and prodict the molar absorption coefficient of a protein. *Protein Science.* 4:2411-2423.

Permyakov, E. A. 1993. Luminescent Spectroscopy of Proteins, CRC Press, Boca Raton, Florida.

Ravid, S., P. Matsumura, and M. Eisenbach. 1986. Restoration of flagellar clockwise rotation in bacterial envelopes by insertion of the chemotaxis protein CheY. *Proc. Natl. Acad. Sci. USA*. 83:7157-7161.

Rebbapragada, A., M. S. Johnson, G. P. Harding, A. J. Zuccarelli, H. M. Fletcher, I. B. Zhulin, and B. L. Taylor. 1997. The Aer protein and the serine chemoreceptor Tsr independently sense intracellular energy levels and transducer oxygen, redox, and energy signals for *Escherichia coli* behavior. *Proc. Natl. Acad. Sci. USA*. 94, 10541-10546.

Reinhart, G. D. 1983. The determination of thermodynamic allosteric parameters of an enzyme undergoing steady-state turnover. *Arch. Biochem. Biophys.* 224:389-401.

Reinhart, G. D. 1985. Influence of pH on the regulatory kinetics of rat liver phosphofructokinase: a thermodynamic linked-function analysis. *Biochemistry.* 24(25):7166-7172.

Reinhart, G. D. 2004. Quantitative analysis and interpretation of allosteric behavior. *Methods Enzymol.* 380:187-203.

Riley-Lovingshimer, M. R. and G. D. Reinhart. 2005. Examination of MgATP binding in a tryptophan-shift mutant of phosphofructokinase from Bacillus stearothermophilus. *Arch. Biochem. Biophys.* 436(1):178-186.

Segall, J. E., S. M. Block, and H. C. Berg. 1986. Temporal comparisons in bacterial chemotaxis. *Proc. Nat. Acad. Sci. USA.* 83:8987-8991.

Shimizu, T. S., N. Le Novere, M. D. Levin, A. J. Beavil, B. J. Sutton, and D. Bray. 2000. Molecular model of a lattice of signaling proteins involved in bacterial chemotaxis. *Nat. Cell Biol.* 2:792-796.

Silverman, M. and M. Simon. 1974. Flagellar rotation and the mechanism of bacterial motility. *Nature.* 249:73-74.

Smith, P. K., R. I. Krohn, G. T. Hermanson, A. K. Mallia, F. H. Gartner, M. D. Proyenzano, E. K. Fujimoto, N. M. Goeke, B. J. Olson, and D. C. Klenk. 1985. Measurement of protein using bicinchoninic acid. *Anal. Biochem.* 150:76-85.

Solovyova, A. S., M. Nollmann, T. J. Mitchell, and O. Byron. 2004. The solution structure and oligomerization behavior of two bacterial toxins: pneumolysin and perfringolysin O. *Biophys. J.* 87(1):540-552.

Sourjik, V. and H. C. Berg. 2002. Receptor sensitivity in bacterial chemotaxis. *Proc. Natl. Acad. Sci. USA.* 99(1):123-127.

Springer, M. S., M. F. Goy, and J. Adler. 1977. Sensory transduction in *Escherichia coli*: two complementary pathways of information processing that involve methylated proteins. *Proc. Natl. Acad. Sci. USA.* 74:3312-3316.

Stock, A., T. Chen, D. Welsh, and J. Stock. 1988. CheA protein, a central regulator of bacterial chemotaxis, belongs to a family of proteins that control gene expression in response to changing environmental conditions. *Proc. Natl. Acad. Sci. USA.* 85(5):1403-1407.

Stock, A. M. and J. B. Stock. 1987. Purification and characterization of the CheZ protein of bacterial chemotaxis. *J. Bacteriol.* 169(7):3301-3311.

Stock, J. B., A. M. Stock, and J. M. Mottonen. 1990. Signal transduction in bacteria. *Nature.* 344(6265):395-400.

Stock, J. B. and M. G. Surette. 1996. chemotaxis. In *Escherichia coli* and *Salmonella typhimurium*, 2nd. Neidhardt, F. C, Stock, J. B., and Surette, M. G. (eds). Washington DC: American Society for Microbiology Press, 1103-1125.

Surette, M. G., M. Levit, Y. Liu, G. Lukat, E. G. Ninfa, A. Ninfa, and J. B. Stock. 1996. Dimerization is Required for the Activity of the Protein Histidine Kinase CheA that Mediates Signal Transduction in Bacterial Chemotaxis. *J. Biol. Chemistry.* 271:939-945.

Toews, M. L., M. F. Goy, M. S. Springer, and J. Adler. 1979. Attractants and repellents control demethylation of methylated chemotaxis proteins in *Escherichia coli. Proc. Natl. Acad. Sci. USA*. 76:5544-5548.

Tso, W.W. and J. Adler. 1974. Negative Chemotaxis in Escherichia coli. *J. Bacteriol.* 118(2):560-576.

Turner, L., W. S. Ryu, and H. C. Berg. 2000. Real-time imaging of fluorescent flagellar filaments, *J. Bacteriol.* 182:2793-2801.

Vissavajjhala, P. and A. H. Ross. 1990. Purification and characterization of the recombinant extracellular domain of human nerve growth factor receptor expressed in a baculovirus system. *J. Biol. Chem.* 265:4746-4752.

Weber, G. 1972. Ligand binding and internal equilibrium in proteins. *Biochemistry.* 11:864-878.

Weber, G. 1975. Energetics of ligands binding to proteins. *Adv. Protein. Chem.* 29:1-83.

Wyman, J. 1967. Allosteric linkage. *J. Am. Chem. Soc.* 89:2202-2218.

Weerasuriya, S., B. M Schneider, and M. D. Manson. 1998. Chimeric chemoreceptors in Escherichia coli: signaling properties of Tar-Tap and Tap-Tar hybrids. *J. Bacteriol.* 180:914-920.

Weinryb, I. and R. F. Steiner. 1971. The luminescence of the aromatic amino acids. *Excited States of Proteins and Nucleic Acids*, R. F. Steiner and I. Weinryb (eds.), *Plenum Press, New York***.** pp. 277-318.

Welch, M., K. Oosawa, S. Aizawa, and M. Eisenbach. 1993. Phosphorylation-dependent binding of a signal molecule to the flagellar switch of bacteria. *Proc. Natl. Acad. Sci. USA*. 90:8787-8791.

Wyman, J. 1964. Linked functions and reciprocal effects in hemoglobin: a second look. *Adv. Protein Chem.* 19:223-286.

Yeh, J. I., H. P. Biemann, J. Pandit, D. E. Koshland, and S. H. Kim. 1993. The three-dimensional structure of the ligand-binding domain of a wild-type bacterial chemotaxis receptor. Structural comparison to the cross-linked mutant forms and conformational changes upon ligand binding. *J. Biol. Chem.* 268:9787-9792.

Yeh, J. I., H. P. Biemann, G. G. Prive, J. Pandit, D. E. Koshland Jr., and S. H. Kim. 1996. High-resolution structures of the ligand binding domain of the wild-type bacterial aspartate receptor. *J. Mol. Biol.* 262(2):186-201.

Zukin, R. S. 1979. Evidence for a conformational change in the *Escherichia coli* maltose receptor by excited state fluorescence lifetime data, *Biochemistry.* 18:2139-2145.

VITA

LIN FAN
Lab of Dr. Gregory D. Reinhart; Department of Biochemistry & Biophysics
103 Biochemistry/Biophysics Building; Texas A&M University
2128 TAMU; College Station, Texas 77843-2128
(979) 739-7075
us_fanlin@yahoo.com

EDUCATION

Texas A&M University, College Station, TX 2005
M.S., Biochemistry

Louisiana Tech University, Ruston, LA 2002
M.S., Chemistry

Guangzhou University of Traditional Chinese Medicine 1998
Guangzhou, Guangdong, China
B.S., Pharmacy

AWARDS

Graduate Teaching Award, Texas A&M University 2004-2005